Chapter 8
Reactive Power Compensation in AC Power Systems

Ersan Kabalci

Abstract This chapter introduces most widely used reactive power compensators considering the recent advances seen in industrial applications. In order to provide better and deeper knowledge for authors, the basic principles of reactive power compensation and symmetrical systems are presented primarily. The theoretical backgrounds are discussed by comparing each approach and application types in detail. The remainder of the chapter is organized by considering the comprehensive figure that is illustrated in the third section. Thereby, the first generation conventional compensators and lately improved FACTS are introduced in the following sections. Furthermore, the compensation devices are also listed according to their integration to transmission line as shunt, series, and shunt-series devices. The circuit diagrams and control characteristics of each compensation device are presented with its analytical expressions. The power flow control, voltage and current modifications, and stability issues are illustrated with phasor diagrams in order to create further knowledge on operation principles for each device. The comparisons are associated with similar devices and emerging technologies.

8.1 Introduction

This chapter deals with reactive power definition, analytical background, and compensation methods applied for reactive power. The reactive power compensation is also known as VAR compensation in several textbooks. The VAR compensation implies the volt-ampere-reactive that is unit of the reactive power. The demands of lower power losses, faster response to parameter change of the system, and higher system stability have stimulated the development of the flexible ac transmission systems (FACTS) that stands for compensation systems connected to the transmission line in series or shunt. Besides the series and shunt connections of

E. Kabalci (✉)
Department of Electrical and Electronics Engineering, Faculty of Engineering and Architecture, Nevsehir HBV University, Nevsehir, Turkey
e-mail: kabalci@nevsehir.edu.tr

controllers, the most comprehensive compensators are implemented with semi-conductor converters based on multilevel topologies.

The static synchronous compensator (STATCOM) that is usually defined as self-commutated or static VAR compensator is a voltage source converter (VSC) based on controllable switches to control the reactive power Q continuously. Furthermore, STATCOM is shunt connected to the utility grid or system at the point of common coupling (PCC). The maximum value of Q is adjusted relatively to the voltage, and the maximum available Q is slightly decreased when the voltage is decreased. Thus, the instability of the voltage causes imbalances on Q. The load current consists of three components as active power (P), reactive power (Q), and harmonic contents where the demanded current should be purely sinusoidal and in phase with the line voltage. The STATCOM also eliminates harmonic contents of the generated voltage and current waveforms by using several control methods and topological configurations.

The multipulse converters are developed using the most widely known six-pulse configurations. The variations of multipulse converters are built by combining six-pulse converters via phase-shifting isolation transformers. On the other hand, multilevel converters were developed as an alternative to the multipulse configurations owing to their multi MVA switching capability that is inherited from series or parallel connection of modular cells. The most widely known topologies of multilevel converters are diode clamped, flying capacitor, and cascaded H-bridge configurations that are also introduced in this chapter. The multilevel converter topologies provide several advantages such as harmonic elimination, lower electromagnetic interference, better output waveforms, and increased power factor correction capabilities together. Furthermore, each switch can be controlled individually to robustly tackle the unbalanced load operations even in higher switching frequencies relatively to the multipulse configuration. The following sections introduce the basic principles of reactive power compensation, the state-of-art in compensator devices, conventional and FACTS compensators. The control and operation characteristics of converters are also surveyed in terms of the main topological issues.

8.2 Basic Principles of Photovoltaic Energy Conversion

8.2.1 Background

The increased energy demand of the power industry has caused several requirements since past a few decades. The distributed generation (DG) and microgrid opportunities that are additionally promoted by renewable energy source (RES) integration have accelerated the growth of conventional grid. Therefore, the number of power plants types and substations, and the length of transmission and distribution lines are increased rapidly than ever before. The most widely installed

Fig. 8.1 The power triangle

$$S = I^2 Z = VI \qquad Q = I^2 X = VI \sin\varphi$$
$$S = \sqrt{P^2 + Q^2}$$
$$\varphi \qquad P = I^2 R = VI \cos\varphi$$
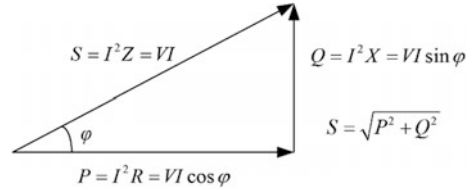
devices to control the conventional grid are mechanic circuit breakers where the response times are quite long to interact rapidly against the frequently changing loads. The loads require electrical or magnetic field to generate the reactive power. The reactive power consumers using inductive power are electrical motors, generators with lagging power factor, transformers, and transmission lines with heavy current loads. The transmission lines without any load or with low-level loads, rectifiers with capacitor filters, capacitors, generators operating at lagging power factor generate reactive power to meet the electrical field requirement where these kinds of loads presents capacitive power.

The electrical power is defined in three types as apparent power S, active power P, and reactive power Q in ac where the apparent power consist of real part P and imaginary part Q as seen in Fig. 8.1.

The equations seen in Fig. 8.1 are depended to impedances where apparent resistance and reactance compose it as follows;

$$Z = R + jX \tag{8.1}$$

where the reactance is depended on the particular frequency under consideration and can be calculated for capacitances or inductances as given in Eq. (8.2), respectively [1–3];

$$X_C = \frac{1}{\omega C}, \quad X_L = \omega L \tag{8.2}$$

The equations given above prove that the reactive power is depended on the reactance where the voltage and frequency are effective parameters. The ac power systems are expected to present constant voltage and frequency at any node under ideal conditions. Furthermore, the total harmonic distortion (*THD*) ratio should be zero and power factor (*PF*) should be unity in an ideal ac power system. The constant frequency is provided by sustaining the balance between generated and consumed power rates that is completely irrespective of voltage.

On the other hand, the voltage plays a vital role on system stability where it can be easily affected by varying reactive power. Thus, it clearly depicts that the focus of reactive power compensation is related to pursuing the system stability for all players in a transmission system, for both of generators and loads. The reactive power compensation is handled in two aspects as load compensation to improve the power quality for individual or particular loads, and transmission compensation that deals with long-distance and high voltage transmission lines [4].

The load compensation is expected to manage three main objectives that are listed as *power factor correction, load balancing,* and *voltage regulation.* The power factor correction minimizes the required reactive power that is met by central power stations. A great part of industrial loads operates at lagging PF that causes reactive power demand to consume. The power factor correction is used to provide the required reactive power locally instead of consuming from utility grid. Therefore, the *PF* of loads are increased up to unity value by decreasing the reactive power demand from utility, and the efficiency and capacity of generating stations are improved that support to sustain voltage stability on the transmission lines.

The *load balancing* is also performed in a similar way to power factor correction in order to decrease the required load current that tends to be higher than required active power rates. Since the higher load current increases joule losses in transmission and distribution lines, the load balancing allows minimizing line losses by this way. The *voltage regulation* is related to maintain utility supply at the allowed limits against rapidly and heavily changing load situations, that cause to voltage dips and flickers. It is based on installing a robust power system including high sized and number of generating units, and interconnecting to construct an intensive network. Since this approach seems high-cost and open to severe faults, the appropriate sizing and reactive power compensation of transmission and distribution lines can carry out another solution. The effect of *PF* on the transmission line losses can be expressed analytically as seen in Eq. (8.3) where the losses are quadratically increased against decreasing *PF*.

$$P_L = \frac{lP^2}{kAV^2(\cos\varphi)^2} \tag{8.3}$$

The parameters given in the equation are;

l	= length of the conductor,
P	= carried active power,
k	= electrical conductivity,
A	= cross-section of the conductor,
V	= line voltage,
$\cos\varphi$	= fundamental frequency *PF*.

The transmission line losses can be decreased to k_{PL} factor by improving the $\cos\varphi$ fundamental frequency PF to $\cos\varphi_1$;

$$k_{PL} = 1 - \left(\frac{\cos\varphi}{\cos\varphi_1}\right)^2 \tag{8.4}$$

where the reactive power compensation in power systems provides to increase system stability by managing the *PF*. The reactive power compensation helps to increase available maximum load of any transmission line to the thermal limits under stability ranges without complex sizing requirements. This is obtained by

using traditional reactive power compensations such as series or shunt capacitors, and variable compensators. On the other hand, the most recent compensation technologies under FACTS group enables to manage system stability relevant to voltage control, power demand control, and transient controls [1, 4].

8.2.2   The Theory of Reactive Power Compensation

The basic relations across the source and load should be realized to comprehend reactive power compensation theory. A pure resistive load as seen in Fig. 8.2a generates a phase difference δ between load voltage V and source voltage E while consuming power. The PF angle φ in a resistive loaded system is zero since that is between V and I. The voltage difference between source and load is expressed with jX_SI that is orthogonal to terminal voltage as shown in Fig. 8.2b.

The pure inductive loaded system and phasor diagram are illustrated in Fig. 8.3 referring to aforementioned approach. The pure inductive loads, i.e. shunt reactors used in tap-changing transformers and generation stations, do not draw power and δ between load voltage V and source voltage E is zero. Since the voltage drop jX_SI is in phase between V and E, the load voltage is easily affected by the inductive load current. This situation is the main reason of the shunt reactors usage to reduce the voltage.

The phasor diagram of the pure capacitive loaded system seen in Fig. 8.4a is opposite to pure inductive load. It also do not draw power and δ between load voltage V and source voltage E is zero as similar to pure inductive loaded system.

The capacitive loads, i.e. shunt capacitors, are used to increase the line voltage in the transmission and distribution lines, and this type of applications are used to
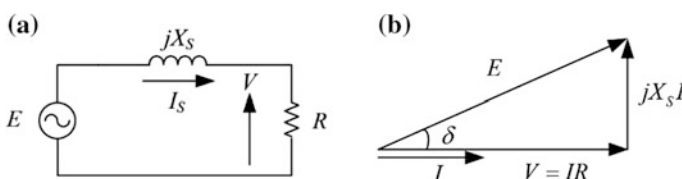

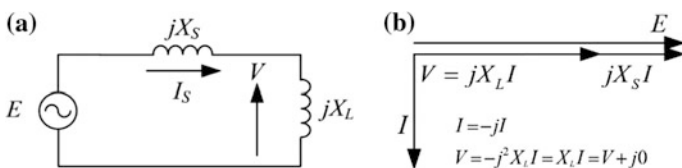Fig. 8.2   Pure resistive loaded system, **a** circuit diagram, **b** phasor diagram

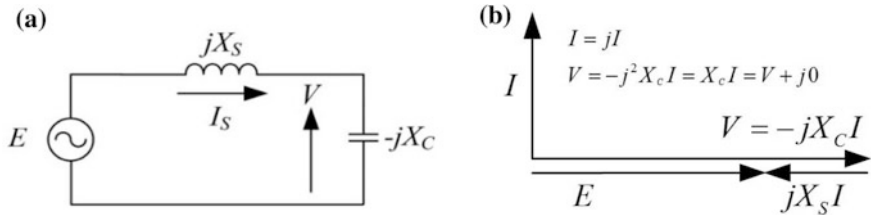Fig. 8.3   Pure inductive loaded system, **a** circuit diagram, **b** phasor diagram

(a)

(b)

$$I = jI$$
$$V = -j^2 X_c I = X_c I = V + j0$$
$$V = -jX_c I$$

Fig. 8.4 Pure capacitive loaded system, **a** circuit diagram, **b** phasor diagram

(a)

(b)

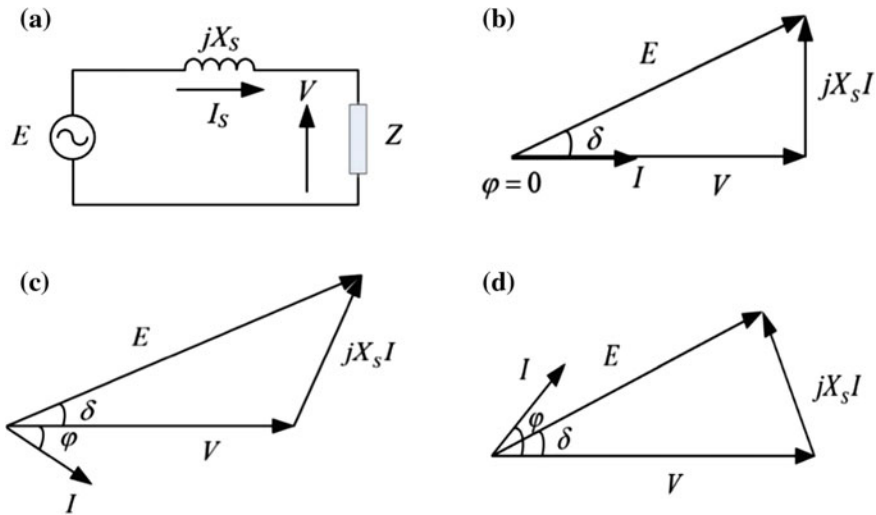**(c)**

(d)

Fig. 8.5 *PF* analyses in an AC system, **a** circuit diagram, **b** resistive load phasor diagram, **c** inductive load phasor diagram, **d** capacitive load phasor diagram

tolerate the tendency to reduce the line voltage under heavy loads [4–6]. The load type defines that the current phasor to be in phase, lagging, or leading to the voltage phasor in an AC system. If we assume a power system installed as seen in Fig. 8.5a with terminal voltage E and transmission line impedance with jX_S, the PF is defined by load type.

In a resistive loaded application of this system, the current and terminal voltage will remain in same phase as seen in Fig. 8.5b where the system operates at unity *PF*. In an inductively loaded system, the current phasor is moved to clockwise as shown in Fig. 8.5c. In this case, the phase angle between current and terminal voltage φ is negative, and the power system operates at lagging PF that requires higher source voltage E for an exact load comparing to unity PF operation. In the third option, the leading PF occurs depending on the capacitive impedance of load where the phase angle between current and terminal voltage φ is positive as seen in Fig. 8.5d. At this operation, the source voltage E required for an exact load is lower than unity PF operation.
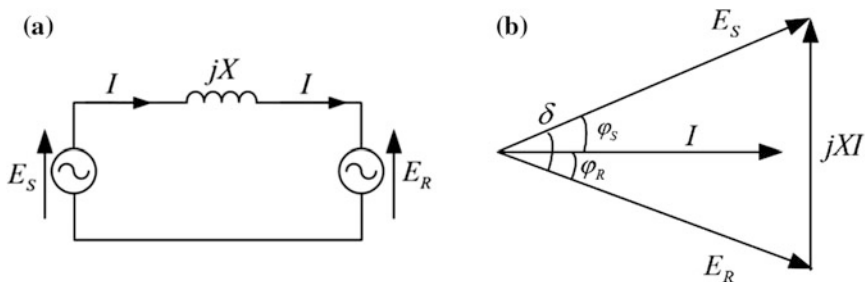
Fig. 8.6 Symmetrical system with source and receptor sections, **a** circuit diagram, **b** phasor diagram

The symmetrical systems where both sides of transmission line are comprised of generators or sources instead of source-load system are one of the most important application area of reactive power compensation. The most basic structure of such a system is illustrated in Fig. 8.6 similarly to pure resistive, inductive, and capacitive loaded systems.

The symmetrical system includes two sources at each side of transmission line where the basic definitions are done as source voltage E_S and receptor voltage E_R. However, this simple model can be assumed as generation stations connected over a line with jX impedance. Although the system may include several industrial loads, they are not considered in this power system since the main concern is directed to power exchange between generators. The bi-directional power flow is analyzed regarding to source voltage E_S, receptor voltage E_R, impedance X, and phase angle among voltage phasors δ as follows;

$$P = \frac{E_S E_R}{X} \sin \delta \qquad (8.5)$$

Besides the phase angle δ, there are two PF angles for each terminal voltages where φ_S denotes the phase angle between source voltage E_S and I phasor while φ_R depicts the phase angle between receptor voltage E_R and I phasor [4, 6–8].

The basic idea of compensation is based on ideal shunt or ideal series compensators that constitute a lossless power system among the generators and loads connected over a transmission line as expressed in symmetrical system. The operation of an ideal shunt compensator consisting of capacitors compensates the power system by conditioning the PF angle where its operating principle is explained referring to Fig. 8.7. A symmetrical system and a shunt compensator integrated to the system at the middle of the transmission line is illustrated in the figure where source and receptor impedances (Z_S, Z_R), line parameters ($jX_{S/2}$), voltages at PCC with phase angles (E_S, E_R, δ_1, δ_2) are indicated. The shunt compensator connected in the middle of the transmission line is a voltage source that is continuously controlled where E_S and E_R sources supply same magnitude and phase angles are defined by the degrees of δ_1 and δ_2. Furthermore, voltage and phase
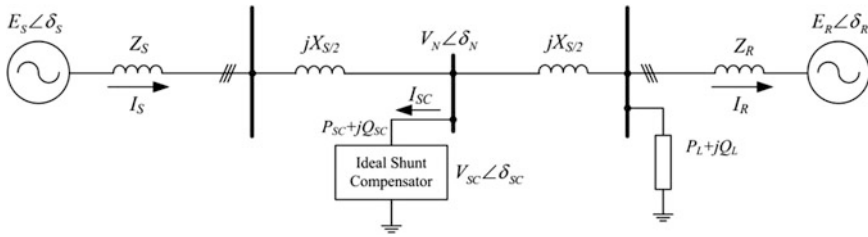
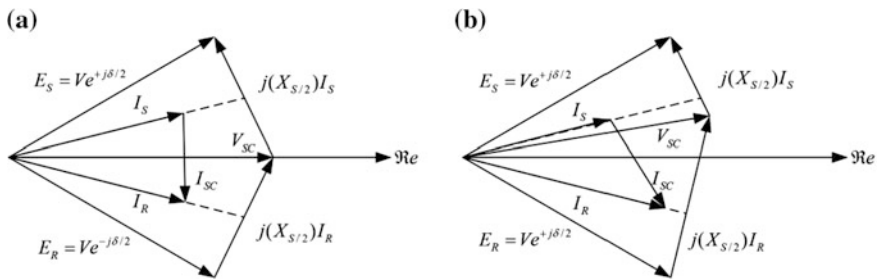**Fig. 8.7** Ideal shunt compensator connection to the symmetrical system

Fig. 8.8 Phasor diagrams of ideal shunt compensator, **a** reactive power compensation, **b** reactive and active power compensation

angles of the shunt compensator are expressed with V_{SC} and δ_2 as seen in the middle of the circuit diagram. The voltage and its phase angle at the node connection are depicted with V_N and δ_N.

The phasor diagrams of the symmetrical system with shunt compensation is depicted in Fig. 8.8 where the phase angles of E_S and E_R are assumed as $(+\delta/2)$ and $(-\delta/2)$, respectively. The phase angles indicate that I_S current flows from first source to the line while I_R flows from line to second source, namely receptor. The I_{SC} phasor that is orthogonal to the V_{SC} as seen in Fig. 8.8a shows the obtained current along the shunt compensator where it means the compensator does not consider the active power P for generation or consuming. In this case, the compensator only draws reactive power Q at the terminal connections. The power transferred from E_S to E_R is calculated as seen in Eq. (8.6) by assuming that there is not any P exchange between line and shunt compensator,

$$P_1 = \frac{2E^2}{X_S} \sin(\delta/2) \tag{8.6}$$

where the P_1 is the active power flowing from E_S source while E is the vector sum of E_S and E_R sources. The drawn power would be at the rate of calculated value of Eq. (8.7), if there is not any compensation is performed in the power system.
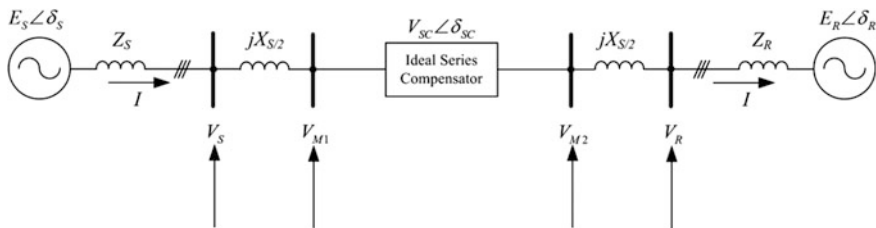
Fig. 8.9 Ideal series compensator connection to the symmetrical system

$$P_1 = \frac{V^2}{X_L}\sin(\delta) \qquad (8.7)$$

Since $[2\sin(\delta/2)]$ is ever greater than $\sin\delta$, that is in the range of $[0, 2\pi]$, the control capability of line is increased by the compensator. When the phase angles of E_S and E_R differ from $\delta/2$, active and reactive power components are generated in the power exchange through sources as shown in Fig. 8.8b. In this situation, the shunt compensator should be operated to adjust any of P or Q owing to its power electronics based structure. Furthermore, the device structure also varies according to requirement of P or Q compensation since they have opposite phasor characteristic caused by the stored energy type [6–9].

The ideal series compensator that is connected to the transmission line in series is constituted by a voltage source V_{SC} as shown in Fig. 8.9. The current value that is delivered from source to receptor over transmission line is calculated as follows;

$$I = \frac{(E_{SR} - E_{SC})}{jX_S}, \qquad E_{SR} = E_S - E_R \qquad (8.8)$$

The series compensator utilizes capacitor banks to minimize the overall reactance of a transmission line at the line frequency where the reactance balance is arranged by the reactive power of capacitors. The reactive voltage that is generated by capacitors provides to improve phase angle and voltage stability in addition to load sharing optimization.

The phasor diagrams of the symmetrical system with ideal series compensation is depicted in Fig. 8.10 where the phase angles of E_S and E_R are assumed as $(+\delta/2)$ and $(-\delta/2)$, respectively. The series compensator does not generate or consume any active power when the compensator voltage V_{SC} is generated orthogonal to the line current I. The power type of the series compensator is just reactive power and the reactance is balanced by using capacitive or inductive impedances. The equivalent impedance X_{eq} is calculated by

$$X_{eq} = X_S(1 + k) \qquad (8.9)$$
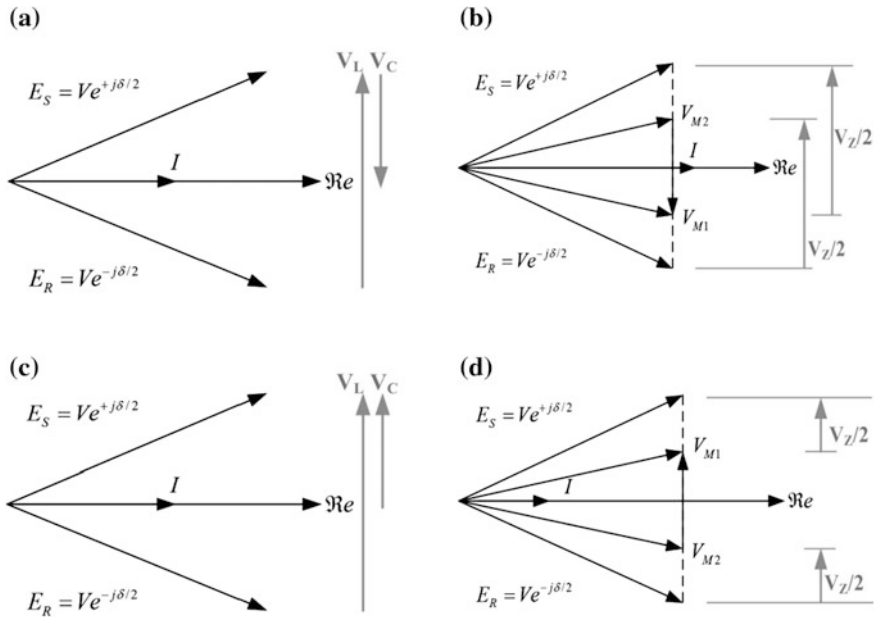
(a)

(b)

(c)

(d)

Fig. 8.10 Phasor diagram of ideal series reactive compensator; **a** capacitive operation without compensation, **b** capacitive operation with compensation, **c** reactive operation without compensation, **d** reactive operation with compensation

$$k = \frac{X_C}{X_S}, \quad 0 \leq |k| \leq 1 \tag{8.10}$$

where X_C is the series compensation reactance. The compensation factor k is positive at the inductive reactance and negative at the capacitive reactance. The compensation voltage V_{SC} and the delivered power are calculated as follows

$$V_{SC} = IX_{eq} \tag{8.11}$$

$$P_S = \frac{V^2}{X_S(1 - k)} \sin \delta \tag{8.12}$$

where the equation depicts that the delivered power can be adjusted by selecting the proper k factor. Similarly, the reactive power delivered by series compensator to receptor is determined as seen in Eq. 8.13;

$$Q_S = \frac{2V^2 k}{X_S(1 - k)^2} (1 - \cos \delta) \tag{8.13}$$

The phasor diagram of the symmetrical system seen in Fig. 8.9 is illustrated in Fig. 8.10a without any series compensation. The voltage phasor V_S corresponding to the line reactance X_S, and the compensation voltage phasor V_C are expressed on the right of Fig. 8.10b for an exact compensation value. The phasor of line current I leads to the compensation voltage V_C by 90° at this situation. In this case, the voltage drop occurred on the line $V_Z = E_C - E_S - V_C$ is greater than the regular voltage drop V_L. The compensation process increases the current flowing on the line according to the situation before compensation that proves the series compensation is essential to increase the delivered power.

The same symmetrical system without compensation is shown in Fig. 8.10c where the series inductive compensation is given in Fig. 8.10d. The phase difference of compensation voltage phasor V_C and drop voltage phasor V_L are 0° that provides generating lower equivalent voltage drop V_Z comparing to capacitive compensation seen in Fig. 8.10b in this case. This process causes to generating lower current to flow on the transmission line where the delivered power level is decreased. In any application of series compensation, capacitive or inductive, there is not any active power is generated or drawn.

The active power transfer characteristic according to power angle δ is illustrated in Fig. 8.11 in a transmission line where the cases are surveyed to compare the line without any compensation, with shunt compensation, with series compensation, and phase-shift compensation. The assumptions are performed regarding to Figs. 8.7 and 8.9, where the compensation factor of series compensator k is adjusted to 50% (0.5) regarding to Eq. (8.9).

The shunt compensator is not used to increase the power transfer capability in its regular operation angle that is originally lower than 90° and is usually around 30°. In case increasing the power is required the series compensation is the most appropriate selection as Fig. 8.11 depicts.
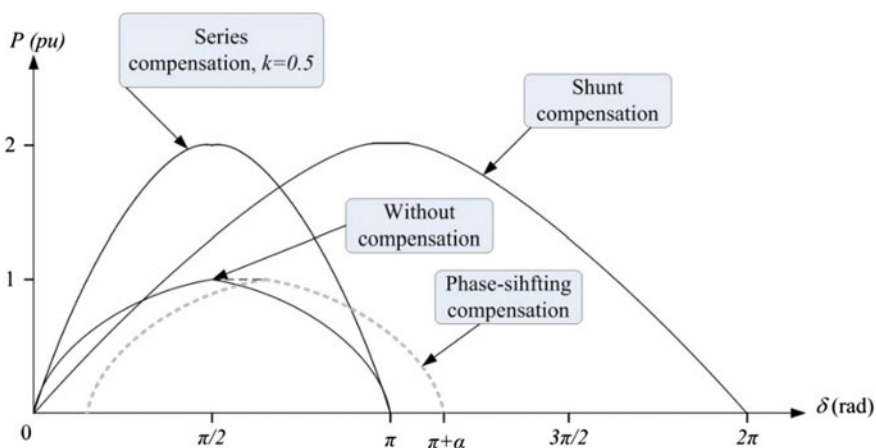

Fig. 8.11 Power transfer characteristics for several compensation cases

The most important supplement of shunt compensator is to increase the power stability of the system. The phase-shifting compensator has a great potential for symmetrical systems under exceeding or unpredictable phase differences. It is preferred to stabilize the phase fluctuations instead of increasing the power [6, 9–11].

8.2.3 Devices Used in Reactive Power Compensation

The FACTS originated from several reactive power compensators propose extensive use of power electronic devices and systems in ac power control. There are several FACTS devices are proposed and being studied since 1990. The first generation conventional compensators were constituted of inductive and capacitive reactive elements to build shunt, series, and shunt-series compensators as illustrated in Fig. 8.12. The improvements of power semiconductors promoted new device types and synthesizes of circuit topologies depending the capabilities of semiconductors. The aggregated terms of FACTS include several device types as seen on the right hand side of Fig. 8.12 where the commutation style is one of the most
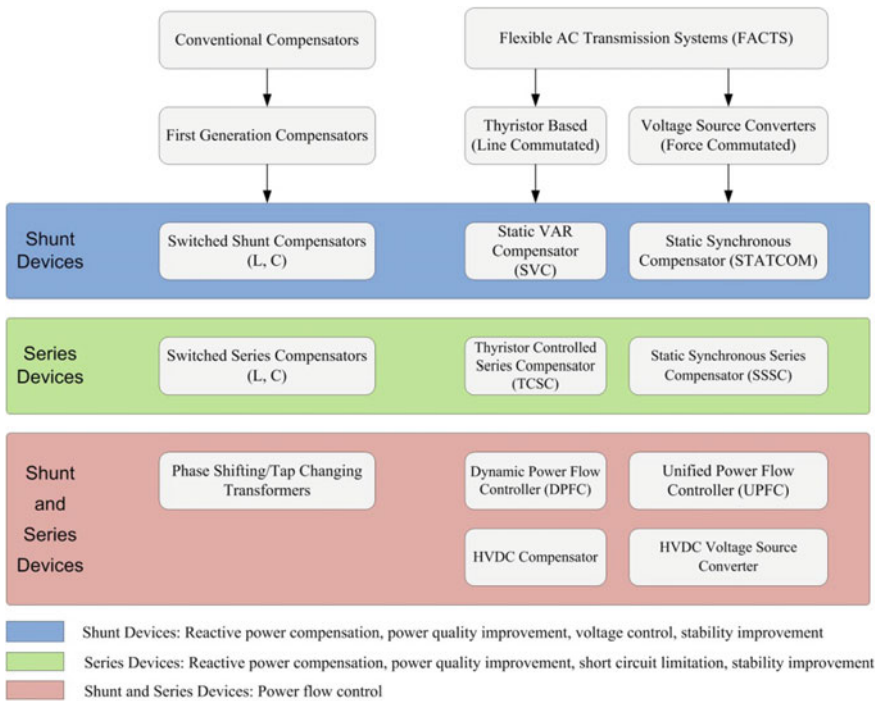

Fig. 8.12 A comprehensive list of FACTS devices

widely accepted indicator to classify device topologies. The connection type to the transmission line is another significant indicator to detect the usage of FACTS.

The essential application areas of FACTS are power flow control, voltage control, VAR compensation, stability improvement in terms of phase and voltage, power conditioning, and interconnection of several sources in distributed generation. The connection type to the transmission line and semiconductors of compensators involve several different operating characteristics. The conventional compensators are constructed with static components such as diodes, inductances, capacitances, and mechanic controllable devices such as tap-changing transformers.

The modern FACTS devices are installed by using more sophisticated components as thyristors or bi-directional semiconductors such as gate turn-off thyristors (GTOs), insulated gate bipolar transistors (IGBTs) or insulated gate commutated thyristors (IGCTs). The thyristor-based topologies are known as line commutated due to unidirectional switching property of the device is depended to the half-cycle polarity of the line. However, the advanced technology of bi-directional switches allow commutating the FACTS at the desired period of entire cycle [4, 6, 7, 12]. In this case, voltage source converters (VSCs) generate completely controllable output in terms of magnitude and phase angle owing to pulse width modulation (PWM) methods used to control IGBTs or IGCTs. The PWM frequency is freely adjusted to decrease THD ratio of the generated output voltage and compensate the power quality of the transmission line. Therefore, particular designs can be carried out in terms of device topology and commutation methods [6, 11–14].

The line commutated FACTS devices can be listed as thyristor-switched capacitor (TSC), thyristor-controlled reactor (TCR), static VAR compensator (SVC), thyristor-controlled series compensator (TCSC) that all are based on aforementioned ideal shunt or series compensator methodology as shown in Fig. 8.12. The right hand side of FACTS listed in Fig. 8.12 includes VSCs with advanced technologies of STATCOM, static synchronous series compensator (SSSC), unified power flow controller (UPFC)), dynamic power flow controller (DPFC) and HVDC VSCs. The FACTS improve the stability and power quality by adapting to rapidly changing line situations and dynamically responding even at the voltage dip and flicker cases.

The illustration given in the figure is also coloured in order to express application aims of compensators regarding to particular requests. The reactive power compensation and voltage control is primarily performed by selecting shunt devices that are shown in the first line of the figure. The SVCs are capable to present more accurate and smoother control comparing to mechanically switched shunt compensators. In this case, the STATCOM is the most recent and the most robust shunt compensator device comparing to others. The series devices shown in green box are preferred to compensate the line stability and reactive power depending to its adaptive impedance feature. These devices are implemented according to TSC, TCR, and SVCs where the main difference is their series connection to the transmission line. In the most cases, the series compensators are used a thyristor by-pass in order to protect the compensator.

The TCSC provides a controllable capacitance to perform power flow control and oscillation damping among the sources and loads. The TCSC is a quite effective device against the damping problems occurred during the integration of large power systems, and they can more accurately overcome similar problems than SSSC device that is not contemporarily being used in the transmission lines since their higher costs.

Furthermore, the TCSC prevents the of sub-synchronous resonance (SSR) problem that is seen as an interaction between heat based generating systems and series compensated systems. One of the most significant application areas of series compensators is seen in distribution lines of industrial plants against voltage dips and flickers. These special devices are known as dynamic voltage restorer (DVR) or static voltage restorer (SVR) [6, 11, 13–18].

The most extensively researched and improving compensation devices designed in shunt and series connection to perform power flow control. These are shown in red box of Fig. 8.12 as a new line. The increased energy demand requires dynamic and balanced power flow control between overloaded units and spare power systems of transmission line. The phase shifting or tap changing transformers (PST) are the first generation devices of shunt-series compensators.

As it is easily realized, the lower response speed, lower control ability, and periodic maintenance requirements of these devices are their drawbacks comparing to semiconductors. The unified power flow controller (UPFC) is a more sophisticated and convenient compensator owing to its fast and dynamic structure. It can be assumed as a composition of a STATCOM and an SSSC using common dc link for power flow control. The dc link is generated by a small capacitor connected between STATCOM and SSSC where the STATCOM draws active power and SSSC generates power at the same ratio to balance the transmission line.

The main drawback of this installation is its high cost caused by power semiconductors used in both devices. The dynamic power flow controller (DPFC) that is a combination of one traditional PST and a SSSC/thyristor switched series reactor (TSSR) is improved to tackle this situation by providing a simpler device to perform the same issue with low cost. The DPFC provides more dynamic performance than a traditional PST where it controls the reactance by a set of thyristors integrated to the transmission line serially. It is capable to control the active and reactive power delivered through the transmission line. Depending on the reactive power requirements of the system, the DPFC configuration is implemented by using a mechanically switched shunt capacitor (MSC) [6, 7, 11, 14].

The high voltage direct current (HVDC) compensators are associated with FACTS in industrial applications as shown in Fig. 8.12. HVDC and FACTS experienced researches and improvements primarily based on thyristors and recently based on bi-directionally controlled semiconductors. The power converters defined as back-to-back (B2B) systems can be built up with thyristors or bi-directional semiconductors such as IGBT, IGCT where they allow to the complete control of power flow while the thyristor based topologies controls only the active power. Although the drawbacks of thyristor devices, the VSCs based on HVDC B2B systems are capable to decouple frequency at the both sides of

symmetrical systems. Furthermore, many PWM control methods decreasing THD and electromagnetic interference (EMI) are implemented owing to advantages of recent power semiconductors.

The HVDC and FACTS are fully or are partially integrated in many applications. It is noted that there are more than a hundred HVDC power plants are installed in worldwide, delivering more than 80 GW power. The current source converters (CSCs) alternatively to VSCs find application areas in power systems especially at 1000 MW and over. However, they are assumed as a mature technology since thyristor based configurations. The CSCs are naturally resistant against short circuits since the series inductor helps to limit inrush currents appearing at faulty operations while VSCs are weaker at line faults. The dc circuit breakers and cable are more attractive for VSC HVDCs in this case [7, 13–16].

8.3 Conventional Equipment for Reactive Power Compensation

The VAR compensators based on generating are classified into two groups as rotating and static generators. The antecedent applications of shunt capacitor and shunt inductor as power flow controllers (PFCs) are dated to 1914. The power semiconductors have attracted the improvement of static VAR compensators starting from last half of previous century. Then, the thyristor switched capacitors and reactors are improved to utilize rapid and dynamic response of power electronic devices. Afterwards, they are associated with tap-changing and PSTs that is the most reliable way to control the delivered power on the parallel transmission lines. The PFCs such as PSTs and series compensators were widely used in steady-state operation of transmission line that the technique is implemented by observing the effect of compensator on the power flow. The technique lying behind PST compensation is its unique and different design criteria comparing to regular power transformers. It can be produced as two-core or single-core symmetrical/asymmetrical constructions.

The power flow control based on PST can be performed by adjusting the phase-shift angle δ_C between source and receptor sides of symmetrical system as seen in power controller plane in Fig. 8.13. This method is used to determine steady-state conditions of the transmission line where the delivered active power is compensated by PFC [11, 19, 20–25].

The power controller plane is used to detect the power limits of the transmission line and the compensator. The bounded area is called the "operating area" depicting all operating points of the PFC to ensure operation is limited in the steady-state. The first generation compensators based on capacitor or inductors were arranged regarding to steady-state assumptions. However, the widely fluctuating loads expose the power system to large reactive power variations. In this case, the fixed capacitor banks lack to compensate the reactive power leading to
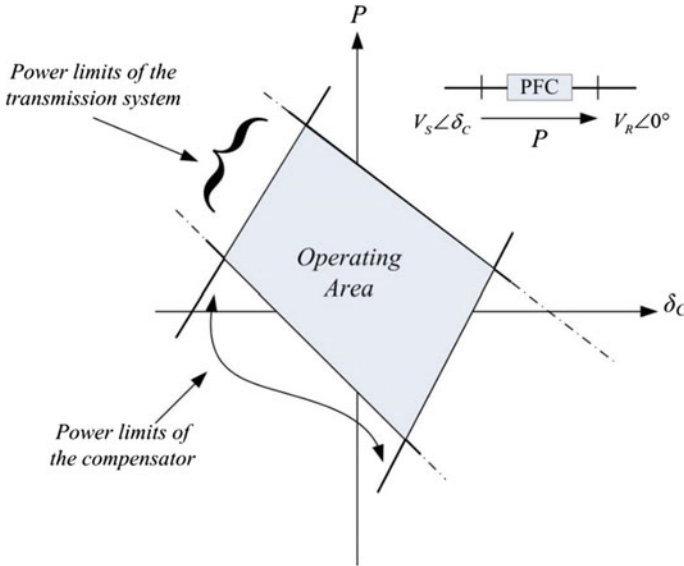
Fig. 8.13 Operating area of a power flow controller (PFC) in the power controller plane

over-compensation or under-compensation. The switched capacitor and reactors are proposed to tackle this drawback by providing variable compensation owing to variable switching angle. The primary switching applications were being performed using mechanical switches such as relays and circuit breakers that are replaced with power semiconductors lately [6, 9, 11].

8.3.1 Thyristor Switched Capacitor (TSC)

The TSC is shown in Fig. 8.14a that is constructed with a line transformer, bi-directional thyristor valve, and a capacitor where a small inductance can be added in series to limit the current. Either the SVCs are defined with switched or control as previously expresses TSC and TCR. The switching term is used to emphasize that the thyristors are turned on at the exact angles only when zero-voltage switching (ZVS) condition is achieved for TSC. The voltages at the thyristor terminals are kept at zero in ideal conditions. However, the required positive amplitude across anode to cathode for switching thyristors is provided in practice, and thyristor valve provides connection and disconnection of capacitors to the line. In the case of a small reactor is preferred to use, it should be located among the transformer and thyristor valve to prevent inrush currents under critical conditions.
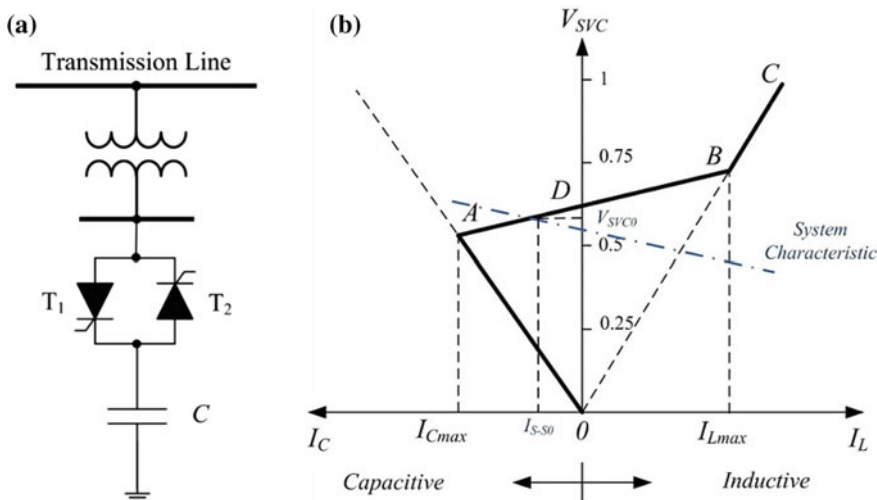
Fig. 8.14 Thyristor switched capacitor, **a** circuit diagram, **b** control characteristic of SVC

The thyristor valve is closed in case of steady-state conditions and TSC is connected to the transmission line where it is imposed to handle sinusoidal ac line voltage. The TSC current at this interval is

$$I_{S-S} = V \frac{n^2}{n^2 - 1} \omega C \cos \omega t \qquad (8.14)$$

where V is the terminal voltage of TSC and n is given by

$$n = \frac{1}{\sqrt{\omega^2 LC}} = \sqrt{\frac{X_C}{X_L}} \qquad (8.15)$$

The current flowing across the capacitor at a given interval t is determined by the following where it is assumed that the equivalent resistance of the TSC is nearly zero comparing to the transmission system;

$$i(t) = \frac{V_m}{X_C - X_L} \cos(\omega t + \alpha) - \frac{V_m}{X_C - X_L} \cos(\alpha) \cos(\omega_r t)$$
$$+ \left[\frac{X_C V_m \sin(\alpha)}{\omega_r L (X_C - X_L)} - \frac{V_{CO}}{\omega_r L} \right] \sin(\omega_r t) \qquad (8.16)$$

$$\omega_r = \frac{1}{\sqrt{LC}} \qquad (8.17)$$

where V_m is the instantaneous maximum voltage of the source, X_C and X_L are capacitive and inductive reactance of the compensator, α is the phase-shift angle of voltage when the capacitor is connected to the line, ω_r is the resonance frequency, and V_{C0} is the capacitor voltage at $t = 0^-$

Since the capacitor voltage V_{C0} is equal to source voltage, the current component of the TSC will be zero when the capacitor is connected at the peak value of source voltage V_m, ($\alpha = \pm90°$). When the TSC is disconnected from line, the capacitor will be charged to the source voltage and remains at this value. In case the capacitor voltage is protected at the maximum peak value, the TSC can be switched again without any fluctuation. Furthermore, the reconnection of capacitor to the line may be done between zero and peak V_{C0} [6, 11, 15].

The steady-state control characteristic of SVC seen in Fig. 8.14b represents the control area on the line of ADB. The 0A line depicts the maximum limit of capacitor while BC line shows the maximum inductor limit in terms of voltage and current values. It should be noted that the SVC current is positive while the susceptance is inductive. Thus,

$$I_{S-S} = -B_{SVC}V_{SVC} \tag{8.18}$$

The slope of 0A line is determined by the susceptance of the capacitor B_C, while the slope of OBC line depends on susceptance of the reactor B_L. A positive slope in the range between 1–5% is presented to allow shunt operation of several SVCs connected to the same transmission line, and to prevent the operating at the lower and higher limits.

The steady-state degree of SVC line voltage is detected regarding to the system parameters and control features. The system characteristic seen in Fig. 8.14b with a negative slope is given by

$$V_{SVC} = V_{Th} - X_{Th}I_{S-S} \tag{8.19}$$

where V_{Th} and X_{Th} are the Thevenin voltage and reactance calculated from the SVC side to line as follows;

$$V_{Th} = \frac{V \cos(\delta/2)}{\cos(\delta/2)} \tag{8.20}$$

$$X_{Th} = \frac{Z_n}{2}\tan(\theta/2) \tag{8.21}$$

where Z_n is the surge impedance given by [26]

$$Z_n = \sqrt{\frac{L}{C}} \tag{8.22}$$

8.3.2   *Thyristor Controlled Reactor (TCR)*

The TCR is the most widely used compensator with thyristor that is constituted of a line transformer, a bi-directional thyristor valve, and an inductor as seen in Fig. 8.15a. In many cases, the compensator includes LC passive filter configured with fixed values to eliminate particular harmonic orders. The TCR provides frequently variable inductive reactance to the line owing to its shunt connection and controlled phase-angle. The voltage and current waveforms of the compensator are shown in Fig. 8.15b where it is controlled at switching angle α, which increases or decreases the fundamental magnitude of reactor current I_L. The switching angle α, can be adjusted to any degree from 90° to 180° starting from zero crossing interval of voltage. The reactor is completely connected to the line at 90° and is completely disconnected from line at 180° while the partial value connection is available between both cases. The equivalent admittance of a TCR as a function of the switching angle α is shown in Fig. 8.15c where it is depended on the partial connection and disconnection cases.

When the switching angle is increased, the reactor current is decreased and provides to reduce the absorbed reactive power by increasing the equivalent
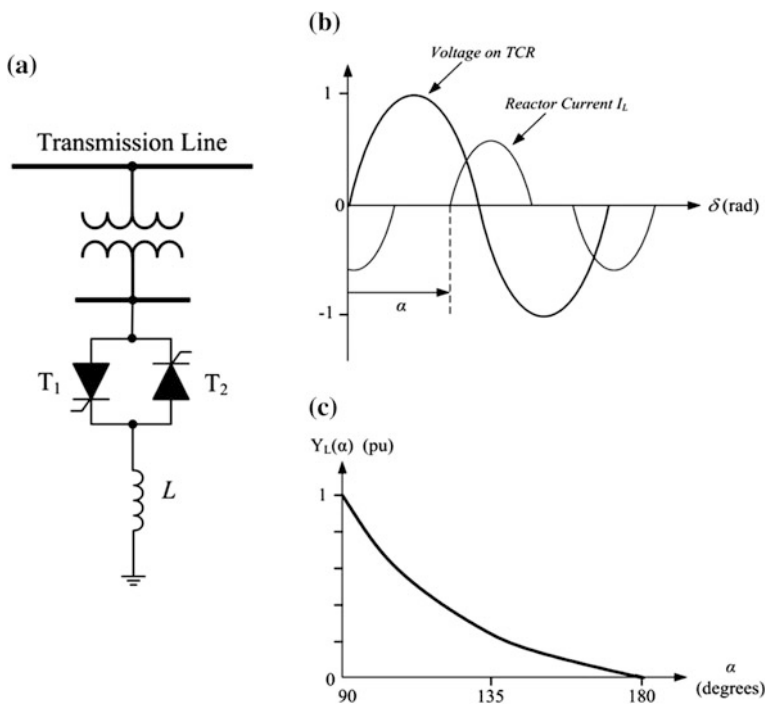

Fig. 8.15 Thyristor controlled reactor, **a** circuit diagram, **b** voltage and current waveforms, **c** equivalent admittance of a TCR as a function of the switching angle α

inductance. The reactor current is calculated depending on inductor and switching angle as given by

$$I_{TCR} = \frac{V_{rms}}{\pi \omega L}(2\pi - 2\alpha + \sin(2\alpha)) \tag{8.23}$$

The TCR compensators provide continuous control, maximum delay limited to one cycle at most, and very low transients during connection and disconnection. However, the significant drawback of the compensator is higher losses in inductive operation areas, and low ordered harmonics of current. The magnitude of current harmonics are defined as shown in Eq. (8.24)

$$I_k = \frac{4V_{rms}}{\pi X_L}\left[\frac{\sin(k+1)\alpha}{2(k+1)} + \frac{\sin(k-1)\alpha}{2(k-1)} - \cos(\alpha)\frac{\sin(k\alpha)}{k}\right] \tag{8.24}$$

where k is harmonic orders; k = 3, 5, 7,... [6, 11, 15, 27, 28].

8.3.3 Thyristor Controlled Series Compensator (TCSC)

The thyristor-controlled series compensator (TCSC) is shown in Fig. 8.16. This compensator is implemented regarding to series connection of a TCR to the transmission line. In the series connection case, a capacitor should be shunt connected to TCR in order to control the current. The most significant advantage of TCSC is balance the damping occurred while integrating large power systems, and to overcome SSR. The circuit diagram seen in figure is identical to regular SVC that is shunt connected to the line.

The TCSC presents two particular principles that are variable capacitive reactance and variable inductance. Both of these principles are managed by TCSC switching methods that are used to control the thyristor valve. Consequently, this configuration provides a continuously controlled series capacitor. The equivalent
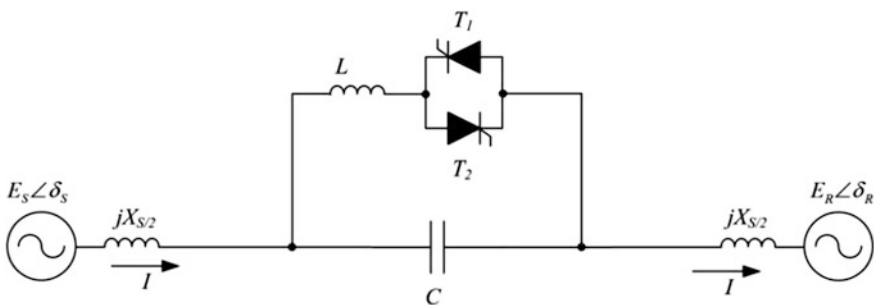

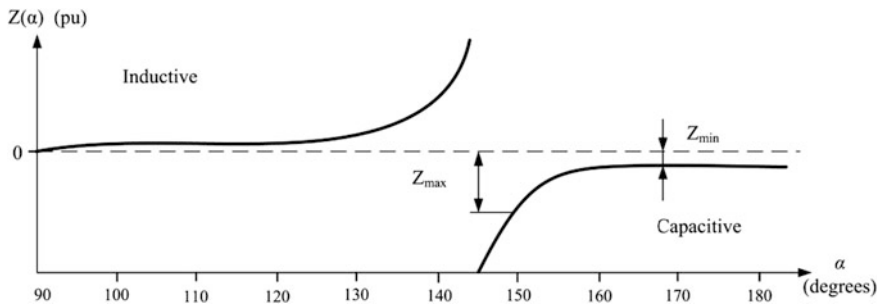**Fig. 8.16** Thyristor controlled series compensator

Fig. 8.17 Equivalent resistance of TCSC as a function of the switching angle α

resistance of TCSC is depicted in Fig. 8.17 as a function of the switching angle α where it is operated in two different areas as inductive and capacitive. The transition between operation ranges appears at around 145° in this case. The regular operation of TCSC is performed in capacitive area up to 180° that the minimum impedance is obtained around this angle. The maximum impedance Z_{max} is presented at 150° switching angle where the resonance around this area is not considered safe for operating.

The TCSC can also be operated in inductive region that is performed by limiting the switching angle between 90° and 140°, where the α lower than 90° causes to decrease the amount of the delivered power [6, 11].

8.4   Flexible AC Transmission System (FACTS)

The force-commutated or self-commutated compensators are implemented by using VSC in order to provide more flexible and robust compensation comparing to conventional line-commutated compensators. The FACTS are integrated to symmetrical systems in shunt, series, or shunt-series connections as conventional compensators and SVCs. The most widely used FACTS are STATCOM and SSSCs where the each compensator is based on VSC to generate compensating voltage and increase the system stability. The most significant contribution of FACTS is harmonic elimination capability that is provided by the sophisticated device configurations and control algorithms.

The improvement of high-power VSCs is promoted by the development of force-commutated semiconductors such as GTOs, IGBTs, and IGCTs. The primary applications of VSCs are shown in Fig. 8.18 where two-level six-pulse VSC is illustrated in Fig. 8.18a and three-level diode clamped topology is shown in Fig. 8.18b. The VSCs are configured with GTOs and antiparallel diodes in order to provide bi-directional current flow where the switches could be IGBT or IGCT. The voltage blocking capability of the VSCs given in the figure is unidirectional. In case of CSCs used, the voltage blocking capability is shifted to bi-directional while the

Fig. 8.18 VSC topologies used in FACTS, **a** basic six-pulse two-level VAR compensator, **b** basic three-level VAR compensator
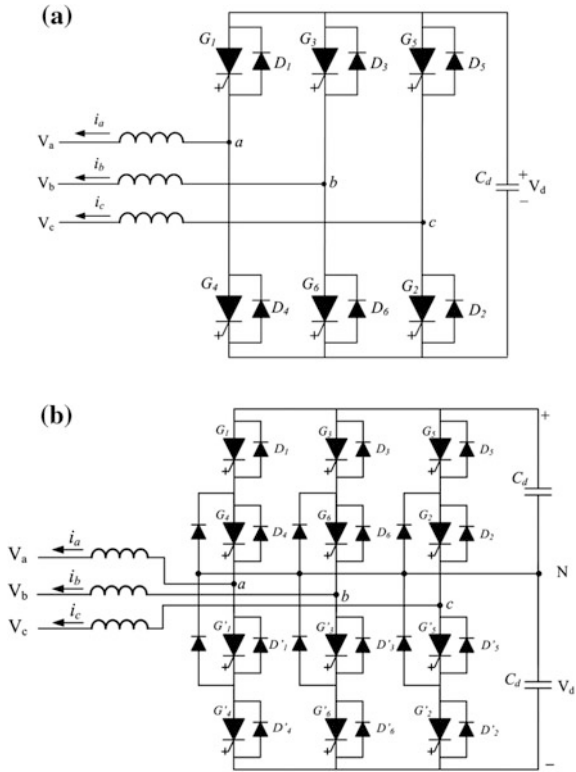
current flow is performed in unidirectional mode. The regular operation of VSC is performed with a voltage source connected to the dc side that allows only reactive power compensation in a compensator application by replacing the dc source with a capacitor [6, 9, 11, 14].

However, in case that active power management is also required, then the circuit involves a small reactor on the ac side of compensator to limit the inrush currents and current spikes during the transients. The first installation of high-power VSC configured in six-pulse topology with 10 MW rated power is done in Japan, in 1991 [6, 11, 29]. The switching frequency was in the line frequency to ensure the stability of the compensator, and eight sets of six VSCs were building a 48-pulse VSC compensator with 80 MVA compensation capability. The ensuing applications of force-commutated VSCs have presented effective compensations and the researches on VSC accelerated their integration to industrial plants.

The emerging power systems and FACTS require more effective controllers such as STATCOMs, (SSSC, UPFC), the inter-phase power controller (IPC), the thyristor-controlled braking resistor (TCBR), the thyristor-controlled voltage limiter (TCVL), the battery energy storage system (BESS), and the superconducting magnetic energy storage (SMES) systems [30].

8.4.1 Static Synchronous Compensator (STATCOM)

A STATCOM is a VSC based compensating device that is shunt connected to the transmission line. A STATCOM integrated to the line and shunt to generators and load operates by generating or absorbing reactive load to compensate the transmission line. The operation principle of STATCOM makes it either a source or a load for the transmission line by replacing widely known series or shunt FACTS. The STATCOM increases the power quality by performing several compensations such as dynamic voltage control, oscillation damping of power line, pursuing the stability during transients, flicker and sag-swell controls, and active and reactive power (PQ) control in transmission systems. Furthermore, STATCOMs substitute SVC devices in the distribution systems [4, 6, 30].

Figure 8.19a shows the basic connection of STATCOM to transmission line where the reactive power control is performed by controlling the terminal voltages.

Fig. 8.19 STATCOM, **a** circuit diagram of line integration, **b** control characteristic of STATCOM
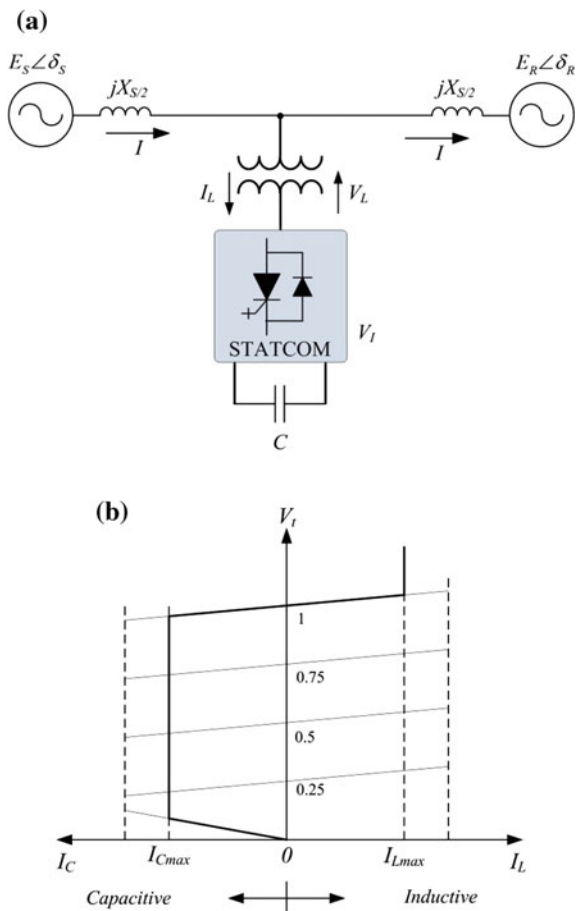
The transmission line is configured in symmetrical system that E_S denotes the source voltage, while the line impedance X_S, line voltage V_L, line current I_L, and receptor voltage E_R are indicated. The reactive power is controlled depending on the compensator voltage V_I control by assuming that is in phase with the source voltage E_S. There are three options to determine the reactive power of STATCOM according to correspondence among the source and STATCOM voltages. In case of equality, there is not any active or reactive power generated or absorbed in STATCOM. When the source voltage exceeds, than the reactive power of STATCOM is shifted to inductive. In the case of the source voltage is lower than STATCOM voltage, this causes to capacitive reactive power.

A typical *V-I* characteristic of STATCOM as shown in Fig. 8.19b, illustrates this situation where the STATCOM can perform inductive or capacitive compensation regarding to its line current. Besides, the V-I characteristics show that STATCOM provides fully capacitive or inductive power starting from lower voltages even from 0.15 p.u.

Thus, the main case that should be handled in reactive power compensation by using STATCOM is to control the magnitude of compensator voltage V_I. This operation is performed based on two basic principles where one is used in multi-pulse converters and the other one for PWM controlled multilevel converters. The capacitor voltage building the dc line can be fixed to a stable magnitude in PWM control of multipulse converter based STATCOM where the compensator voltage is controlled by the modulator. This is managed by adjusting the switching angle owing to PWM modulator. The second STATCOM configuration based on multilevel converters should control the capacitor voltage only to sustain its constant value. The control methods can be either scalar or vector based in this configuration. Furthermore, the multilevel configuration allows switching with high frequency PWM to decrease THD of reactive components [6, 9, 14]. The following sections are dedicated VSC topologies used in STATCOMs where multipulse configurations are indicated by 12-pulse and 24-pulse converters. Afterwards, multilevel topologies and controller structures are analysed to compare to multipulse STATCOMs at a glance.

8.4.1.1 Multi-pulse Converter Based STATCOM

The first VSC based STATCOM applications are developed with multi-pulse converters owing to their lower losses and lower harmonic contents comparing to conventional compensators. The multi-pulse converter topologies consist of several six-pulse VSC circuits where a basic VSC STATCOM in the configuration of six-pulse two-level was illustrated in Fig. 8.18a. The switching devices of the system were GTOs that the converter could generate balanced three-phase ac output voltages by using a dc capacitor as the voltage source. The frequency of the output voltage is adjusted by the modulating frequency of GTO switches and the phase voltages are coupled to ac grid over an interconnection reactor [9, 31, 32].
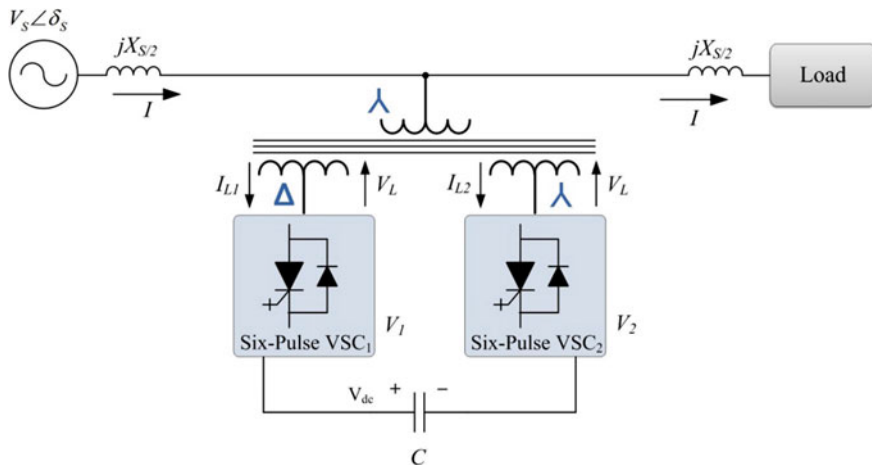
Fig. 8.20 Circuit diagram of two-level 12-pulse STATCOM

The 12-pulse converters are constituted of six-pulse converters connected in parallel as shown in Fig. 8.20. The expressed configuration is improved regarding to two-level topology shown in Fig. 8.18a while another configuration is in three-level structure as illustrated in Fig. 8.18b. The two-level topology requires non-identical winding types for each six pulse VSC that one is Δ-Y connected while other is Y-Y connected to ac grid. The Δ connected secondary of the transformer with three times higher turns according to Y connected secondary provides 30° phase shift comparing to other. Therefore, the lower ordered harmonics are easily eliminated.

The output phase voltage of STATCOM can be calculated by using Eq. (7.25) where n_1 and n_2 are the voltage ratios of the corresponding VSC transformers while v_{a-Y} and $v_{a-\Delta}$ are the output voltages of the Y-Y and Δ-Y connected converters, respectively [9].

$$v_a = n_1 v_{a,Y} + n_2 \frac{v_{a,\Delta}}{\sqrt{3}} \tag{8.25}$$

The voltage magnitude of VSC output depends on modulation index m_i of control signal that allows obtaining the output voltage at $m_i V_{dc}$ where V_{dc} is the voltage across the capacitor. The control signal that is based on some variation of PWM generates switching angle α that generates the STATCOM bus voltage at $V_S \angle \delta_S$ form. The Eq. (8.26) expresses the admittance of transformer

$$Y = \frac{1}{R + jX_S} = G + jB \tag{8.26}$$

that manages the active or reactive power injection to the transmission line. The reactive power generation or absorption ability of STATCOM depends on the control voltage of PWM modulator. The injected reactive power to utility grid is presented as follows

$$Q = V_S^2 B - m_i V_{dc} V_S B \cos(\delta_S - \alpha) + m_i V_{dc} V_S G \sin(\delta_S - \alpha) \qquad (8.27)$$

In case of $V_S > m_i V_{dc}$, Q will be positive that causes STATCOM to absorb reactive power or vice versa [9]. The active power generated by the source to charge the capacitor is expressed as follows,

$$P = \frac{|V_S| m_i V_{dc}}{X_S} \sin(\delta_S - \alpha) \qquad (8.28)$$

The 24-pulse converter topology of STATCOM consists of six-pulse converters where it eliminates the $6n \pm 1$ ordered harmonics. The 23rd, 25th, 47th, and 49th harmonics in the ac output waveform are naturally eliminated since the $n = 4$ for 24-pulse converter. The 24-pulse STATCOM constituting two-level VSCs is illustrated in Fig. 8.21 where this topology is also known as quasi 24-pulse [9, 33]. Each VSC and transformer connection configures a stage that each one is connected to the transmission line by Y-Y and Δ-Y connections of transformers. The transformers may connected in zigzag that generates 15° phase shift according to each other with −7.5°, 7.5°, 22.5°, and 37.5° angles [9, 33, 34].

Another topology of quasi 24-pulse STATCOM is presented in Fig. 8.22 [35] where the VSCs are constituted according to neutral point clamping (NPC) topology that is previously shown in Fig. 8.18b.

The conduction angle α defines the negative and positive cycles of intervals where $\alpha = 180 - 2\beta$, where 2β stands for the dead-band angle. The on-off spectral transitions are ensured by the dead-band angle where the output voltages of a six-pulse three-level VSC is given by Eq. (8.29).
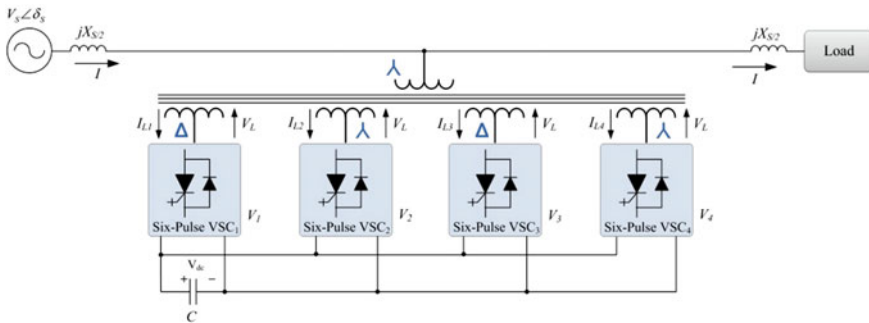

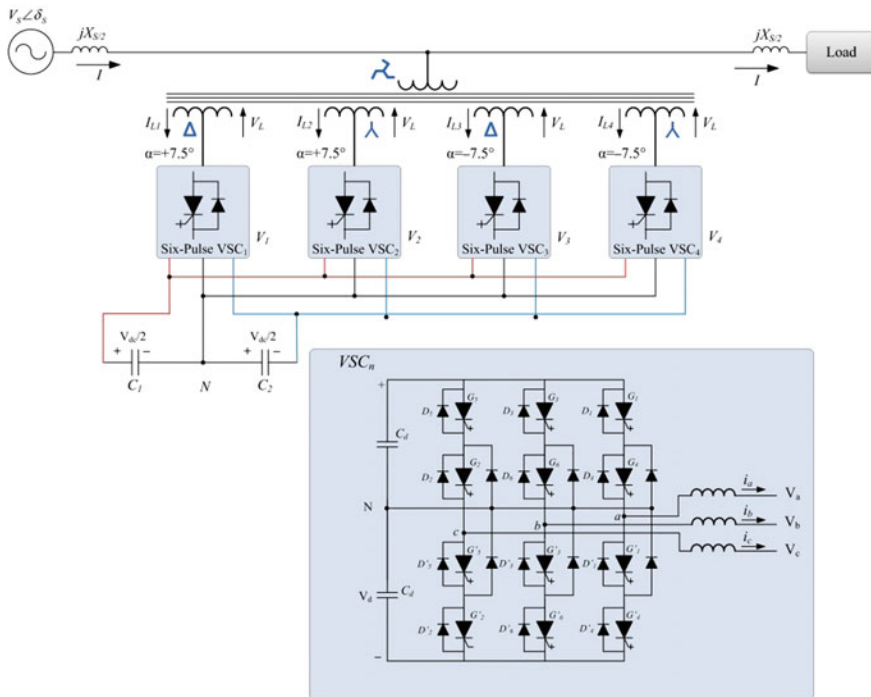Fig. 8.21 Circuit diagram of a quasi two-level 24-pulse STATCOM

Fig. 8.22 Circuit diagram of a three-level 24-pulse STATCOM

$$V_1 = \frac{2\sqrt{6}}{\pi} \frac{v_{dc}}{2} \sin\left(\frac{180 - 2\beta}{2}\right) \tag{8.29}$$

On the other hand, output voltages of a 24-pulse three-level VSC is given as follows while the active and reactive powers are calculated as given below by considering X_S as the reactance along with STATCOM and the transmission line by using Eqs. (8.31) and (8.32) [9, 35]

$$V_{c1} = np\frac{2\sqrt{6}}{6\pi} \frac{v_{dc}}{2} \sin\left(\frac{180 - 2\beta}{2}\right) \cos\frac{\pi}{24} \tag{8.30}$$

$$P = \frac{V_L V_S \sin\delta_S}{X_S} \tag{8.31}$$

$$Q = V_S\left(\frac{V_S - V_L \sin\delta_S}{X_S}\right) \tag{8.32}$$

where the phase angle δ between the ac bus voltage V_S and STATCOM output voltage V_L sustains the dc line voltage V_{dc} at a constant value.

8.4.1.2 Multilevel Converter Based STATCOM

In addition to their power conversion applications, the multilevel converters (MLC) are widely used in active filters, and FACTS. Although the primary applications are improved for medium power ranges, the recent applications have been increased the power range from a few kWs to multi MWs owing to their cascaded topologies. Almost all the three-level STATCOM topologies are implemented with conventional diode clamped (DC) topology where the switching devices were GTOs. This approach indicates that the control strategy of DC is the simplest one among other three-level MLCs in medium and high power application.

The flying capacitor MLC (FC-MLI) that is one of the outstanding topology allows constructing low cost systems, particularly in high power applications, comparing to the DC. However, it involves pre-charge arrangement for the capacitors that are connected through the upper and lower arms. The cascaded H-bridge (CHB) topology is the most recent topology among others that extended its operation area since it provides higher power conversion and lower cost for a given output magnitude level. The CHB consists of several H-bridge cells connected in series to generate multilevel output voltage. One of the most significant features of this topology is higher switching frequency comparing the previous topologies, and increased power rate handled by the total device and equally shared to the each cell. Furthermore, the CHB based STATCOM is capable to eliminate harmonics and to compensate reactive power in superior comparing others.

The main requirement of this configuration is its separated dc sources. However, CHB can be easily integrated to various type of energy sources to obtain higher output levels and energy storage applications [9, 36–39].

Figure 8.23 shows the circuit diagram of STACOM configured by using three-phase five-level CHB including series connection of three-level H-bridge cells at each phase leg. The output voltage synthesis of H-bridges generate a combined phase voltage in staircase waveform oscillating in the ranges of $+V_{dc}$, 0, $-V_{dc}$.

Where V_{a1} and V_{a2} voltages of series connected H-bridge cells synthesize the phase voltage V_{an} in a stepped waveform as seen in Fig. 8.24. The positive levels of output voltage are indicated with P_1 and P_2 while the negatives are P_1^1 and P_2^1. Equation (8.33) expresses the Fourier series expansion of the general multilevel stepped output voltage while the transform applied to the STATCOM in Fig. 8.23 is shown in Eq. (8.34), where n represents harmonic order of the output voltage.

$$V_{an}(t) = \frac{4V_{dc}}{\pi} \sum_{n=1,3,5,\ldots}^{\infty} [\cos(n\alpha_1) + \cos(n\alpha_2) + \ldots + \cos(n\alpha_5)] \frac{\sin(n\omega t)}{n} \quad (8.33)$$

The switching angles α_1, α_3,…, α_5 in Eq. (7.33) are selected for the minimum voltage harmonics [36, 40].
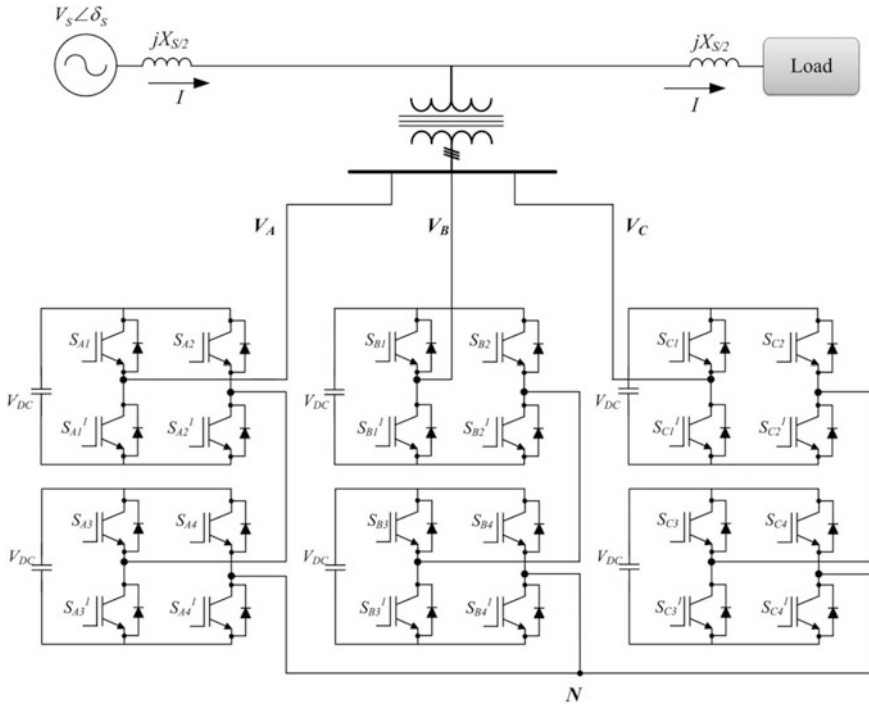
Fig. 8.23 Circuit diagram of a five-level CHB STATCOM

$$V_{an5}(t) = \frac{4V_{dc}}{\pi} \sum_{n=1,3,5,\ldots}^{\infty} [\cos(n\alpha_1) + \cos(n\alpha_2)] \frac{\sin(n\omega t)}{n} \tag{8.34}$$

Researchers have proposed novel MLCs based on hybrid topologies that are based on the existing devices [36, 40].

8.4.2 Static Synchronous Series Compensator (SSSC)

The series capacitor based compensation that brings some capabilities such as increasing the transient stability, reactance control, and load sharing is a conventional technique that was introduced in Sect. 8.3.3. Even though the series compensation is assumed to be used to decrease the reactive impedance of the transmission line, it is actually operated by increasing the line voltage, current, and thereby the delivered power from source to load. Although the mentioned advantages, series compensation has several drawbacks on SSR issues that large energy exchange is done by several sources under synchronous system frequency.
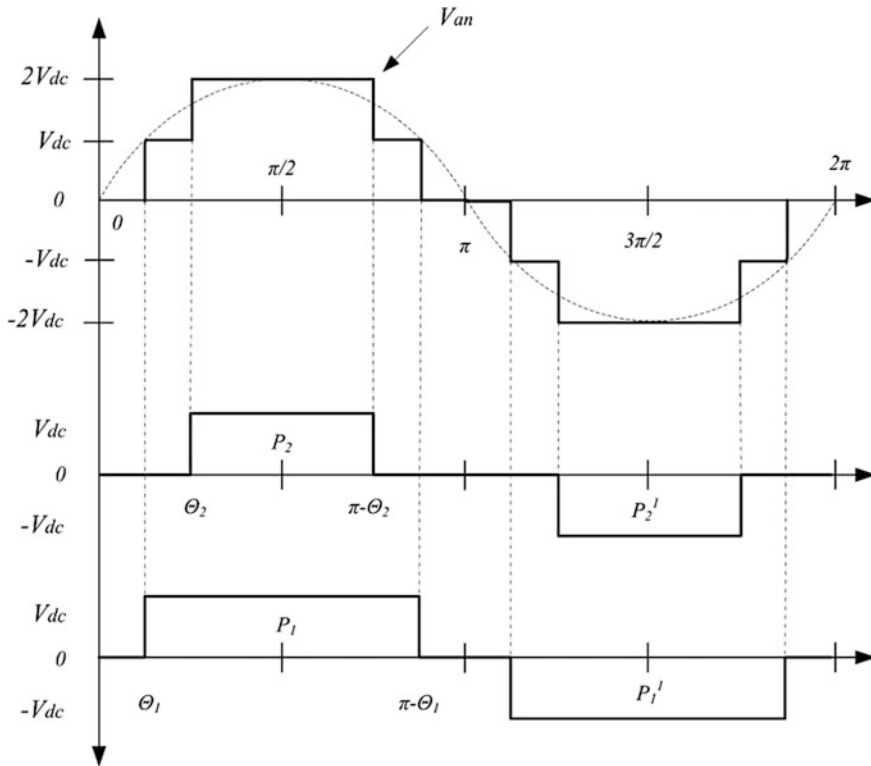
Fig. 8.24 Phase voltage generation of a five-level CHB STATCOM

There are several studies are performed to overcome SSR problem. The robust control methods and configurations of FACTS stand out of other methods proposed by researchers. The SSSC has been developed as an alternative to the TCSC devices where the SSR immunity is inherited from TCSC. In addition to regular advantages of series compensators, SSSC presents numerous capabilities to increase the reactive power control and stability issues. Furthermore, there are several studies are noted that SSSCs effectively damps the SSR comparing regular series compensators [6, 11, 14, 41–46].

Figure 8.25 illustrates basic circuit diagram of a SSSC based on VSC similar to STATCOM that is serially connected to the transmission line, and a capacitor on the dc side. The SSSC controller considers the line current and line voltage to compensate the transmission line by adjusting the reactance in steady-state operation. It should be noted that in case the current is flowing in the line, then SSSC generates compensation voltage V_C that is quadrature to the current and regulates the reactive power demand. The compensation characteristic of the device is same with the one shown in Fig. 8.11 for $0 < \delta < 180°$ during series compensation that yields positive magnitude power delivered.
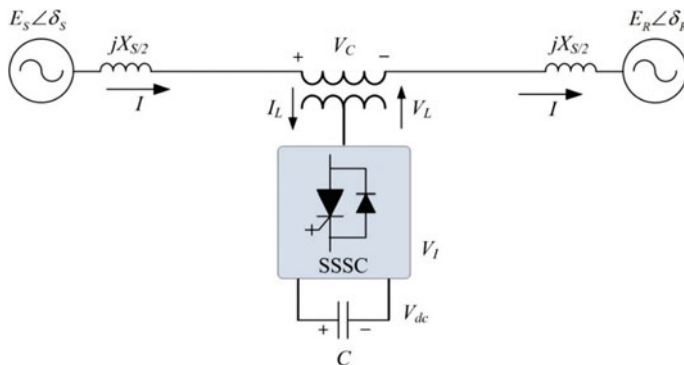
Fig. 8.25   Static synchronous series compensator (SSSC)

The fundamental operating principles of SSSC is compared to conventional series capacitive compensator as shown in Fig. 8.26 where the circuit diagrams for only series compensation with only capacitive compensator (Fig. 8.26a) and with SSSC (Fig. 8.26c), and respective phasor diagrams are analyzed. Despite it is assumed to decrease the line impedance, a series capacitor increases the line voltage, line current, and consequently the power through the line impedance. This approach may be considered irrelevant. However, the voltage along the transmission line is the significant parameter while the capacitor is cared to increase the voltage in order to provide the required current level. The steady-state power transmission can be realized when a synchronous voltage source follows the series compensation as shown in Fig. 8.26c that is analytically presented as follows

$$\overline{V_q} = \overline{V_C} = -jX_C\overline{I} \tag{8.35}$$

It should be noted that there are particular differences between series capacitive compensator and synchronous voltage source type compensator. The operational characteristic of a series capacitor can be illustrated with an ideal voltage source. However, SSSC is significantly different from the series capacitor in terms of delivered power and angle characteristics, active power exchange, and immunity to resonance and SSR, and control ranges.

Capacitor provides reactive impedance that causes proportional voltage to the line current when it is series connected to the line. The compensation voltage is changed regarding to the transmission angle δ and line current. The delivered power P_S is a function of the series compensation degree s where it is given by

$$P_q = \frac{V^2}{X_L(1 - s)}\sin\delta \tag{8.36}$$

where $V = V_1 = V_2$ and $\delta = \delta_1 - \delta_2$. The delivered power P_S regarding to transmission angle δ is shown in Fig. 8.27a as a function of s ($s = 0$, $s = 1/3$, and
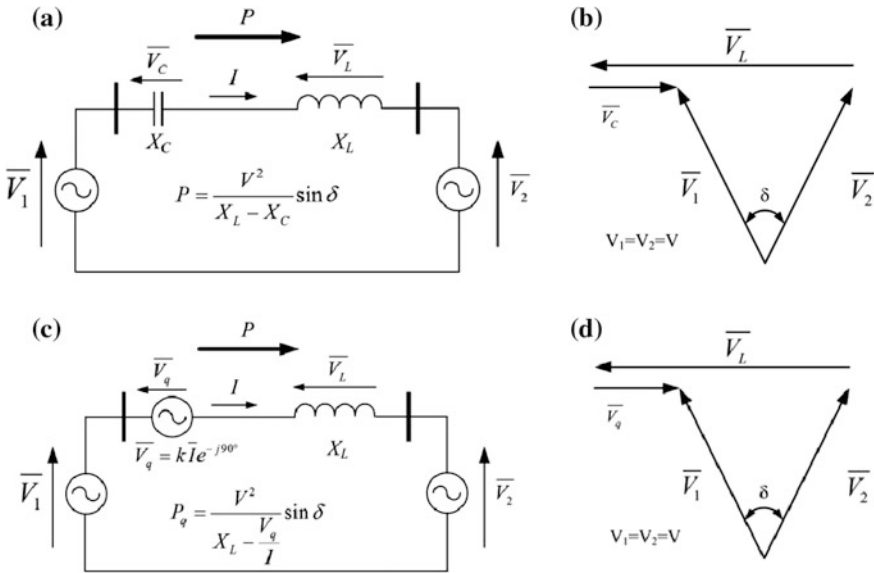
Fig. 8.26 Symmetrical system under series compensating, **a** circuit diagram of series compensating capacitor, **b** phasor diagram of capacitor, **c** circuit diagram of SSSC, **d** phasor diagram of SSSC

$s = 1/5$). Additionally, SSSC is independent from line current while compensating the voltage. The delivered power P_q is a parametric function of injected voltage $V_q = |\overline{V_q}|$ series to line where $\overline{V}_q = V_q[\overline{I}/|\overline{I}|]e^{\mp j90°}$ that is also given by

$$P_q = \frac{V^2}{X_L}\sin\delta + \frac{V}{X_L}V_q\cos\frac{\delta}{2} \qquad (8.37)$$

The delivered power P_q is shown in Fig. 8.27b as a parametric function of injected voltage V_q against transmission angle δ. The normalized V_q voltage is selected to provide same maximum power with series capacitor configuration. The comparison of Fig. 8.27a, b expresses that the series capacitor increases the delivered power by a fixed rate of the delivered by the uncompensated line at a given transmission angle δ. On the other hand, the SSSC increases the delivered power by a fixed fraction of the maximum power available by uncompensated line independent from δ in the angle range of $0 \leq \delta \leq 90°$ [41, 45–47].

8.4.3 Unified Power Flow Controller (UPFC)

The UPFC is a VSC based shunt-series compensator that is constituted of STATCOM and SSSC combination with a common dc link as shown in Fig. 8.28.
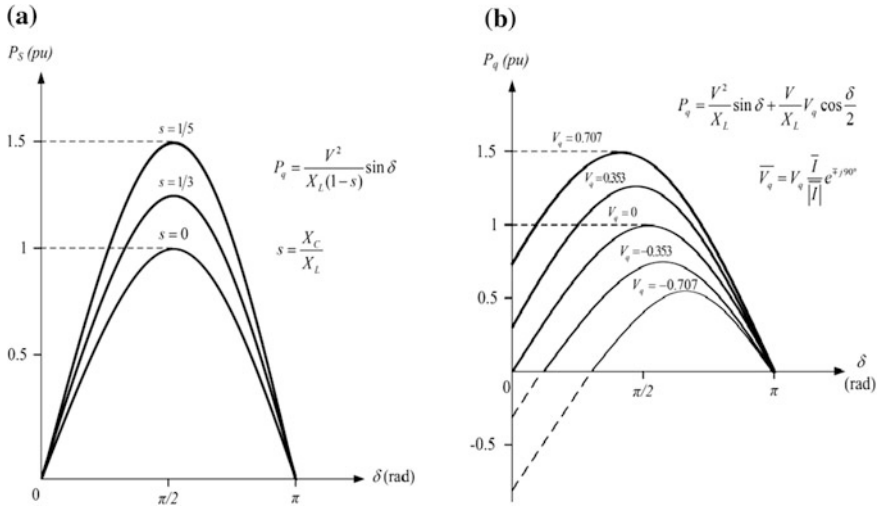
(a)

P_S (pu)

$$P_q = \frac{V^2}{X_L(1-s)} \sin\delta$$

$$s = \frac{X_C}{X_L}$$

s = 1/5

s = 1/3

s = 0

(b)

P_q (pu)

$$P_q = \frac{V^2}{X_L} \sin\delta + \frac{V}{X_L} V_q \cos\frac{\delta}{2}$$

$$\overline{V}_q = V_q \frac{\overline{I}}{|\overline{I}|} e^{\mp j/90°}$$

$V_q = 0.707$

$V_q = 0.353$

$V_q = 0$

$V_q = -0.353$

$V_q = -0.707$

Fig. 8.27 Delivered power P and transmission angle δ relation, **a** series capacitive compensation, **b** SSSC
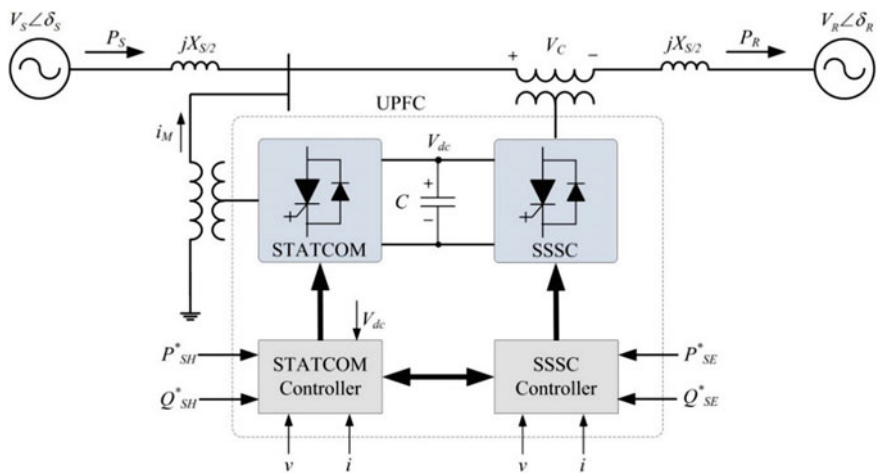

Fig. 8.28 The block diagram of UPFC

Separate observers of each compensator perform the control of UPFC. The shunt and series compensators of UPFC exchange reactive power at the terminals while they are operating as independent FACTS compensators. In this case, SSSC injects a voltage quadrature to the line current, and imitates a series inductive or capacitive reactance to the transmission line. On the other hand, STATCOM injects reactive current in order to imitate shunt reactance to the line while operating stand-alone. In case of the combination as a UPFC), the series compensator voltage can be at any

phase corresponding to the predominant line current. Thereby, the exchanged power can be reactive as well as active power at the terminals of compensators. The active power exchanged by any of the compensators is transmitted to the other compensator across the common dc-link. However, exchanged reactive power is independent from each other compensator.

The controller of STATCOM dynamically adjusts the phase angle between the VSC output voltage and line voltage to get the STATCOM generated or absorbed desired reactive power at the compensation connection. The SSSC can be operated in several modes such as voltage injection, regulation of phase angle, emulation of the line impedance, and automatic power flow control. In any of these applications, SSSC injects a voltage over its series connection to the line. The SSSC can be operated in the same way as examined in the previous section to control active and reactive current. The active power control would fluctuate capacitor voltage that should be observed by STATCOM [6, 11, 14, 26, 47].

The controller of STATCOM dynamically adjusts the phase angle between the VSC output voltage and line voltage to get the STATCOM generated or absorbed desired reactive power at the compensation connection. The maximum value of series voltage V_C is limited by SSSC that is the most significant advantage comparing to thyristor-based compensators. In the case reactive power exchange, the UPFC increases the source voltage V_S while generating reactive power, and decreases while absorbing the reactive power. The power flow of UPFC through the transmission line is analyzed as follows;

$$P_S = P_{sh} + \Re(\overline{V_S I_R^*}) \tag{8.38}$$

$$Q_S = Q_{sh} + \Im(\overline{V_R I_R^*}) \tag{8.39}$$

$$P_R = -\Re(\overline{V_R I_R^*}) \tag{8.40}$$

$$Q_R = -\Im(\overline{V_R I_R^*}) \tag{8.41}$$

where $s_{sh} = \sqrt{3/8} \cdot r_{sh}$. The powers P_{sh} and Q_{sh} absorbed by shunt compensator, and common dc voltages are given by

$$P_{sh} = V_S^2 G_{sh} - s_{sh} V_{dc} V_S G_{sh} \cos(\theta_S - \alpha) - s_{sh} V_{dc} V_S B_{sh} \sin(\theta_S - \alpha) \tag{8.42}$$

$$Q_{sh} = V_S^2 B_{sh} - s_{sh} V_{dc} V_S B_{sh} \cos(\theta_S - \alpha) - s_{sh} V_{dc} V_S G_{sh} \sin(\theta_S - \alpha) \tag{8.43}$$

$$V_{dc} = \frac{P_{sh}}{CV_{dc}} + \frac{\Re(\overline{V_S I_R^*})}{CV_{dc}} - \frac{V_{dc}}{R_C C} - \frac{R_{sh}(P_{sh}^2 + Q_{sh}^2)}{CV_{dc} V_S^2} - \frac{R_{se} I_R^2}{CV_{dc}} \tag{8.44}$$

where G_{sh} is the conductance, and B_{sh} is the susceptance of STATCOM while θ is phase angle of the transmission line and α is the phase angle of the compensator [47].

8.5   State-of-the-Art Equipment for Reactive Power Compensation

8.5.1   Dynamic Power Flow Controller (DPFC)

The DPFC is one of the emerging compensators configured with a standard PST for tap-changing, and several series TSC and TCRs as shown in Fig. 8.29. All the compensators connected in the DPFC are introduced in the previous sections of this chapter. The resulting stepped reactance of DPFC is obtained owing to binary arrangement of reactor and capacitor reactance. The PST controls the phase of transmission line voltage in order to control the power flow across the line. Although the system response of PST is slower since its mechanical configuration, this issue is regulated by rapid structure of TSC and TCR. The series compensators are operated at zero current in order to eliminate harmonic contents. The most significant advantage of DPFC is its lower cost comparing other FACTS.

Furthermore, DPFC has several significant advantages according to PST that are related to the speed of power flow control, and reactive power compensation. The dynamic response of DPFC is quite effective on power oscillation damping (POD) and transient stability in addition to steady-state stability. Furthermore, DPFC is more appropriate in corrective compensation, thereby the system stability and voltage stability is improved owing to its TSC and TCR configuration. This is particularly efficient during overload situations by supporting the transmission line with rapid voltage response. The reactive power consumption of PST is a serious problem in weak grids. DPFC overcomes this issue by compensating the tap-dependency of series inductance, and improves voltage stability [48–50].

The reactance, impedance, and admittance of the transmission line starting from shunt connection of PST a to end of the TCR b are given by;

$$X_{ab} = k_L X_L + k^2 X_E + X_B + X_{Line} - k_C X_C \tag{8.45}$$
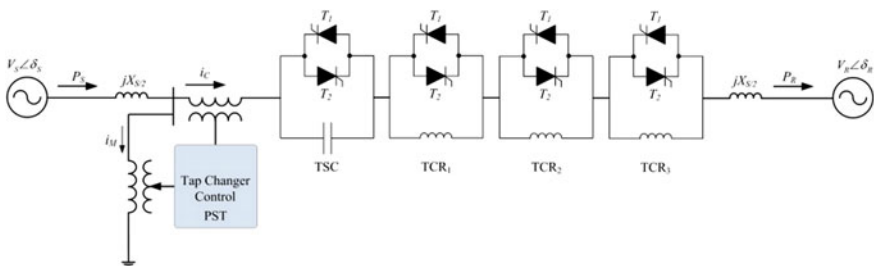
$$Z_{ab} = R_{ab} + jX_{ab} \tag{8.46}$$

Fig. 8.29 The block diagram of DPFC

$$Y_s = Y_{ab} = \frac{1}{Z_{ab}} = G_S + jB_S \qquad (8.47)$$

where $k_L X_L$ and $k_C X_C$ represent the reactive and capacitive modules by ignoring ohmic losses, and k is the PST voltage ratio which is between -1 and 1, X_E, X_B, X_P and R_v are PST internal parameters [51].

8.5.2   VSC-Based HVDC Transmission

The HVDC is an appropriate method used in dc transmission systems. The block diagram of HVDC system is illustrated in Fig. 8.30 that is constituted with VSCs connected B2B. The dc side of converters are coupled with capacitors to regulate the dc line voltage. One of the most significant advantages of VSC based HVDC system is its capability to control active and reactive power separately at each terminal sides that make this system convenient for weak power systems. Furthermore, VSC based HVDC is more effective than CSC on the improvement of system stability and power flow control, and isolation under transients owing to its rapid dynamic response.

The VSC based HVDC can also be used in the interline power flow controller IPFC that is utilized to transfer active power among dc link buses. HVDC system can be seen as an extension of UPFCas well as IPFC in some cases. The main difference between both systems is segmentation of transmission line while HVDC system does, UPFC does not divide.

The HVDC systems with thyristor-based converters control the dc-line current while the most widely used VSC-based configuration controls the dc-line voltage. This difference in the device topology allows using HVDC system in the integration of asynchronous sources. The increased power demand and high rate integration of large distributed sources are handled owing to modular multilevel converter (MMC) based HVDC that is installed by series and parallel connection of VSC cells as shown in Fig. 8.31 [6, 40, 52].

The HVDC systems with thyristor-based converters control the dc-line current while the most widely used VSC-based configuration controls the dc-line voltage. This difference in the device topology allows using HVDC system in the integration
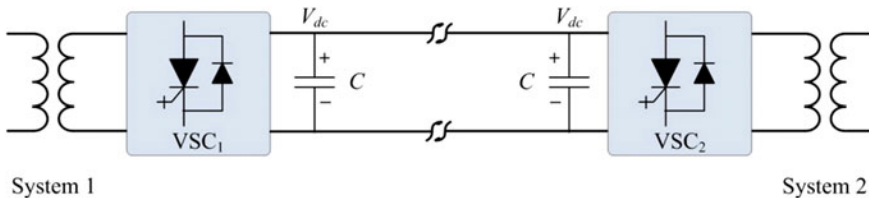

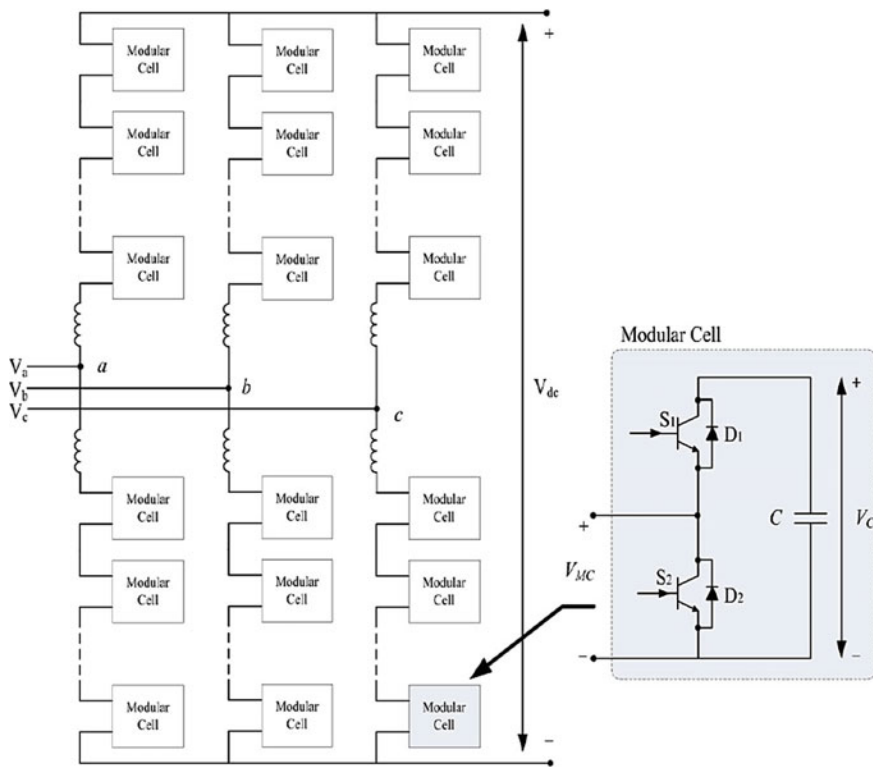Fig. 8.30   The block diagram of HVDC transmission system

Fig. 8.31 The block diagram of MMC based HVDC system

of asynchronous sources. The increased power demand and high rate integration of large distributed sources are handled owing to MMC based HVDC that is installed by series and parallel connection of VSC cells. The most recent applications are performed by MMC topology since its footprint requirements are lower, and capable to control active and reactive power independently. Furthermore, it brings the advantages of lower switching losses, lower dv/dt ratio, modular structure, reconfigurable topology, and direct connection to the power systems without power transformer requirement that decreases the substation area. Besides, MMC configuration provides to use several types of energy storage systems [6, 40, 52].

8.6   Conclusion

The most widely used reactive power compensators in transmission line compensation are introduced in this chapter. The theoretical backgrounds, applications, and compensation methods are discussed in a comprehensive approach by listing the compensator according to their improvements. The shunt devices among others are

being widely used for reactive power compensation and thereby for voltage control. The first improvement seen in compensators is SVCs that are replaced with mechanically switched devices in order to provide more accurate and precise control. The primary contribution of SVC was its rapid and dynamic response to the line fluctuations. However, it was not efficient enough against fast changing power quality problems such as voltage dips and flickers that required the implementation of more robust compensators. The FACTS are improved to overcome this kind of stability problems where the first one was STATCOM listed in the shunt compensator group. In addition to shunt devices, the series compensation devices that are capable to improve line impedance and stability are also considered in FACTS family.

Although the SSSC is a mature technology in series compensation, the TCSC is based on a device that is efficient on damping the SSR and improvement of system stability. However, series VSC based compensators are mostly used in distribution lines instead of transmission lines. The most extensively researched compensators are in shunt-series configurations that are more convenient in power flow control comparing to previous configurations.

The PST are the most common compensators used in power flow control. The drawbacks of this device such as higher footprint and maintenance requirement have promoted the alternative compensators as UPFC), IPFC, and DPFC. Although the UPFC was known for a long time, it is installed for testing and improvement applications. The gap between PST and UPFC) has been fulfilled by DPFC that was meeting the dynamic power flow control requirement with its simpler configuration by overcoming drawbacks of both systems. The most recent compensator responding the industry requirements is VSC-based HVDC compensator. The VSC and MMC configurations brought numerous advantages such as fully independent power control, modular structure, improved voltage and stability control and dynamic power flow control comparing the previous devices.

Although the FACTS are generally recognized as a new technology, there are lots of FACTS are being operated in the industry. The most widely used device is SVC first installed in 1970s and it is known that the total installed SVC compensator capacity is over than 100.000 MVA. It is also noted by literature that over than 700 conventional series compensation plants are installed worldwide that are capable to compensate around 350.000 MVA total power. The successor technologies as VSC-based and MMC HVDC B2B compensators, STATCOM, TSCS, and DPFC present quick improvements in their application areas.

References

1. W. Hofmann, J. Schlabbach, W. Just, Reactive Power Compensation: A Practical Guide, First Edition, John Wiley & Sons Ltd, 2012.
2. P.R. Sharma, A. Kumar, N. Kumar, Optimal Location for Shunt Connected FACTS Devices in a Series Compensated Long Transmission Line, Turk J. Elec. Engineering, vol. 15, no. 3, pp. 321–328, 2007.

3. M. Beza, Control of Energy Storage Equipped Shunt-Connected Converter for Electric Power System Stability Enhancement, Thesis, Department of Energy and Environment Chalmers University of Technology, Gothenburg, Sweden, 2012.
4. E. Acha, V. Agelidis, O. Anaya, T.J.E. Miller, Power Electronic Control in Electrical Systems, Newnes Power Engineering Series, ISBN-13: 978-0750651264, 2002.
5. H. Amaris, M.A. Carlos, A. Ortega, Reactive Power Management of Power Networks with Wind Generation, Lecture Notes in Energy, Springer-Verlag, London, 2013.
6. E.H. Watanabe, M. Aredes, P.G. Barbosa, F.K. de Araujo Lima, R.F. da Silva Dias, G. Santos Jr., 32 - Power Electronic Control in Electrical Systems, Power Electronics Handbook, Third Edition, Edited by Muhammad H. Rashid, Butterworth-Heinemann, Boston, pp. 851–877, 2011.
7. X.P. Zhang, C. Rehtanz, B. Pal, Flexible AC Transmission Systems: Modelling and Control, Springer-Verlag, Berlin, Heidelberg, 2012.
8. T. Petersson, Reactive Power Compensation, ABB Technical Report, no. 500-028E, pp. 1–25, Dec. 1993.
9. F. Shahnia, et al. (Eds.), Static Compensators (STATCOMs) in Power Systems, Springer Science+Business Media, Singapore, 2015.
10. H.K. Tyll, F. Schettle, Historical Overview on Dynamic Reactive Power Compensation Solutions from the Begin of AC Power Transmission Towards Present Applications, Power Systems Conference and Exposition, pp. 1–7, 15–18 March 2009.
11. J. Dixon, L. Moran, J. Rodriguez, R. Domke, Reactive Power Compensation Technologies: State-of-the-Art Review, Proceedings of the IEEE, vol. 93, no. 12, pp. 2144–2164, Dec. 2005.
12. A.A. Edris, et al., Proposed Terms and Definitions for Flexible AC Transmission Systems (FACTS), IEEE Trans. Power Delivery, vol. 12, no. 4, pp. 1848–1853, October 1997.
13. N. Flourentzou, V.G. Agelidis, G.D. Demetriades, VSC-Based HVDC Power Transmission Systems: An Overview, IEEE Transactions on Power Electronics, vol. 24, no. 3, pp. 592–602, March 2009.
14. K. Kalyan, M.L. Sen, Introduction to FACTS Controllers, The Institute of Electrical and Electronics Engineers, Inc., 2009.
15. L. Gyugyi, Power Electronics in Electric Utilities: Static VAR Compensators, Proceedings of the IEEE, vol. 76, no. 4, pp. 483–494, Apr. 1988.
16. L. Liu, H. Li, Y. Xue, W. Liu, Reactive Power Compensation and Optimization Strategy for Grid-Interactive Cascaded Photovoltaic Systems, IEEE Transactions on Power Electronics, vol. 30, no. 1, pp. 188–202, Jan. 2015.
17. H. Akagi, E.H. Watanebe, M. Aredes, Instantaneous Power Theory and Applications to Power Conditioning, IEEE Press, 2007.
18. F.L. Luo, H. Ye, M. Rashid, Digital Power Electronics and Applications, ISBN: 0-1208-8757-6, Elsevier, USA, 2005.
19. J. Brochu, F. Beauregard, J. Lemay, P. Pelletier, R.J. Marceau, Steady-State Analysis of Power Flow Controllers Using the Power Controller Plane, IEEE Transactions on Power Delivery, vol. 14, no. 3, pp. 1024–1031, Jul. 1999.
20. U.N. Khan, T.S. Sidhu, A Phase-Shifting Transformer Protection Technique Based on Directional Comparison Approach, IEEE Transactions on Power Delivery, vol. 29, no. 5, pp. 2315–2323, Oct. 2014.
21. R. Baker, G. Guth, W. Egli, P. Eglin, Control Algorithm for a Static Phase Shifting Transformer to Enhance Transient and Dynamic Stability of Large Power Systems, IEEE Transactions on Power Apparatus and System, vol. PAS-101, no. 9, pp. 3532–3542, Sept. 1982.
22. R. Mihalic, P. Zunko, Phase-Shifting Transformer with Fixed Phase between Terminal Voltage and Voltage Boost: Tool for Transient Stability Margin Enhancement, IEE Proceedings - Generation, Transmission and Distribution, vol. 142, no. 3, pp. 257–262, May 1995.
23. J. Verboomen, D. Van Hertem, P.H. Schavemaker, W.L. Kling, R. Belmans, Analytical Approach to Grid Operation with Phase Shifting Transformers, IEEE Transactions on Power Systems, vol. 23, no. 1, pp. 41–46, Feb. 2008.

24. J. Mescua, A Decoupled Method for Systematic Adjustments of Phase-Shifting and Tap-Changing Transformers, IEEE Transactions on Power Apparatus and Systems, vol. PAS-104, no. 9, pp. 2315, 2321, Sept. 1985

25. Ch.N. Huang, Feature Analysis of Power Flows Based on the Allocations of Phase-Shifting Transformers, IEEE Transactions on Power Systems, vol. 18, no. 1, pp. 266–272, Feb. 2003.

26. K.R. Padiyar, FACTS: Controllers in Power Transmission and Distribution, Anshan Publishers, 1st Edition (August 15, 2009), 978-1848290105.

27. A.K. Chakravorti, A.E. Emanuel, A Current Regulated Switched Capacitor Static Volt Ampere Reactive Compensator, IEEE Transactions on Industry Applications, vol. 30, no. 4, pp. 986–997, Jul./Aug. 1994.

28. H. Jin, G. Goos, L. Lopes, An Efficient Switched-Reactor-Based Static VAr Compensator, IEEE Transactions on Industry Applications, vol. 30, no. 4, pp. 998–1005, Jul./Aug. 1994.

29. S. Mori, K. Matsuno, M. Takeda, M. Seto, Development of a Large Static Var Generator Using Self-Commutated Inverters for Improving Power System Stability, IEEE Transactions Power Delivery, vol. 8, no. 1, pp. 371–377, February 1993.

30. R. Mohan Mathur, R.K. Varma, Thyristor Based FACTS Controllers for Electrical Transmission Systems, ISBN: 978-0-471-20643-9, Wiley-IEEE Press, 2002.

31. B. Singh, K.V. Srinivas, Three-Level 12-Pulse STATCOM with Constant DC Link Voltage, 2009 Annual IEEE India Conference (INDICON), pp. 1–4, 18–20 Dec. 2009.

32. S.R. Barik, B. Nayak, S. Dash, A Comparative Analysis of Three Level VSC Based Multi-Pulse STATCOM, International Journal of Engineering and Technology (IJET), vol. 6, no. 3, pp. 1550–1563, Jun.–Jul. 2014.

33. N. Voraphonpiput, S. Chatratana, Analysis of Quasi 24-Pulse STATCOM Operation and Control Using ATP-EMTP, IEEE Region 10 Conference TENCON 2004, vol. C, pp. 359–362, 21–24 Nov. 2004.

34. B. Singh, R. Saha, A New 24-Pulse STATCOM for Voltage Regulation, Int. Conf. on Power Electronics, Drives and Energy Systems, pp. 1–5, 12–15 Dec. 2006.

35. K.V. Srinivas, B. Singh, Three-Level 24-Pulse STATCOM with Pulse Width Control at Fundamental Frequency Switching, IEEE Industry Applications Society Annual Meeting (IAS), pp. 1–6, 3–7 Oct. 2010.

36. I. Colak, E. Kabalci, R. Bayindir, Review of Multilevel Voltage Source Inverter Topologies and Control Schemes, Energy Conversion and Management, vol. 52, no. 2, pp. 1114–1128, February 2011.

37. I. Colak, E. Kabalci, Practical Implementation of a Digital Signal Processor Controlled Multilevel Inverter with Low Total Harmonic Distortion for Motor Drive Applications, Journal of Power Sources, vol. 196, no. 18, pp. 7585–7593, 2011.

38. I. Colak, E. Kabalci, Developing a Novel Sinusoidal Pulse Width Modulation (SPWM) Technique to Eliminate Side Band Harmonics, International Journal of Electrical Power and Energy Systems, vol. 44, pp. 861–871, 2013.

39. I. Colak, E. Kabalci, Implementation of Energy Efficient Inverter for Renewable Energy Sources, Electric Power Components and Systems, vol. 41, no. 1, pp. 31–46, 2013.

40. D. Soto, T.C. Green, A Comparison of High-Power Converter Topologies for the Implementation of FACTS Controllers, IEEE Transactions on Industrial Electronics, vol. 49, no. 5, pp. 1072–1080, Oct. 2012.

41. L. Gyugyi, C.D. Schauder, K.K. Sen, Static Synchronous Series Compensator: A Solid-State Approach to the Series Compensation of Transmission Lines, IEEE Transactions on Power Delivery, vol. 12, no. 1, pp. 406–417, Jan. 1997.

42. A.C. Pradhan, P.W. Lehn, Frequency-Domain Analysis of the Static Synchronous Series Compensator, IEEE Transactions on Power Delivery, vol. 21, no. 1, pp. 440–449, Jan. 2006.

43. M. Farahani, "Damping of Subsynchronous Oscillations in Power System Using Static Synchronous Series Compensator, IET Generation, Transmission & Distribution, vol. 6, no. 6, pp. 539–544, Jun. 2012.

44. M. Saradarzadeh, S. Farhangi, J.L. Schanen, P.O. Jeannin, D. Frey, Application of Cascaded H-Bridge Distribution-Static Synchronous Series Compensator in Electrical Distribution System Power Flow Control, IET Power Electronics, vol. 5, no. 9, pp. 1660–1675, Nov. 2012.
45. X.P. Zhang, Advanced Modeling of the Multi-Control Functional Static Synchronous Series Compensator (SSSC) in Newton Power Flow, IEEE Transactions on Power Systems, vol. 18, no. 4, pp. 1410–1416, Nov. 2003.
46. R. Benabid, M. Boudour, M.A. Abido, Development of a New Power Injection Model with Embedded Multi-Control Functions for Static Synchronous Series Compensator, IET Generation, Transmission & Distribution, vol. 6, no. 7, pp. 680–692, Jul. 2012.
47. R. Natesan, G. Radman, Effects of STATCOM, SSSC and UPFC on Voltage Stability, Proceedings of the Thirty-Sixth Southeastern Symposium on System Theory, pp. 546–550, 2004.
48. C. Rehtanz, Dynamic Power Flow Controllers for Transmission Corridors, IREP Symposium Bulk Power System Dynamics and Control - VII, Revitalizing Operational Reliability, pp. 1–9, 19–24 Aug. 2007.
49. N. Johansson, Aspects on Dynamic Power Flow Controllers and Related Devices for Increased Flexibility in Electric Power Systems, Royal Institute of Technology School of Electrical Engineering Division of Electrical Machines and Power Electronics, PhD. Dissertation, Stockholm, 2011.
50. U. Hager, K. Gorner, C. Rehtanz, Hardware Model of a Dynamic Power Flow Controller, IEEE Trondheim PowerTech, pp. 1–6, 19–23 Jun. 2011.
51. R. Ahmadi, A. Sheykholeslami, A.N. Niaki, H. Ghaffari, Power Flow Control and Solutions with Dynamic Flow Controller, IEEE Canada Electric Power Conference, EPEC 2008, pp. 1–6, 6–7 Oct. 2008.
52. J. Dorn, H. Huang, D. Retzmann H., Multilevel Voltage-Sourced Converters for HVDC and FACTS Applications, Cigre SC B4 Colloquium, Bergen and Ullensvang, pp. 1–8, Norway, 2009.